Thesis for the Degree

Master of Education

A Numerical Study of a Discontinuous Galerkin Method for Boundary Value Problems

by

Chung-Hwa Lee

Graduate School of Education

Pukyong National University

August 2008

A Numerical Study of a Discontinuous Galerkin Method for Boundary Value Problems

경계값 문제에 대한 불연속 갈레르킨 방법의 수치적 연구

Advisor : Prof. Jun Yong Shin

by

Chung-Hwa Lee

A thesis submitted in partial fulfillment
of the requirement for the degree of

Master of Education

Graduate School of Education
Pukyong National University
August 2008

A Numerical Study of a Discontinuous Galerkin Method for Boundary Value Problems

A dissertation

by

Chung-Hwa Lee

Approved by :

(Chairman) Do Sang Kim

(Member) Jin Mun Jung

(Member) Jun Yong Shin

August 27, 2008

Contents

List of Tables ii

List of Figures v

Abstract(Korean) vii

1. Introduction 1

2. Notations 3

3. A Discontinuous Weak Formulation 5

4. Numerical Experiments 9

   4.1. Homogeneus Neumann Boundary Conditions 9

   4.2. Homogeneus Mixed Boundary Conditions 34

5. Conclusions 45

References 47

Typeset by $\mathcal{A}\mathcal{M}\mathcal{S}$-TEX

List of Tables

Table 4.1. The computed L^2 norm of $u-u_h$ in Case 1-1 when $u(x) = (x-x^2)^2$, $p = 1, 2$, and $N = 5, 10, 20, 40, 80$. 26

Table 4.2. The computed L^2 norm of $u-u_h$ in Case 1-2 when $u(x) = (x-x^2)^2$, $p = 1, 2$, and $N = 5, 10, 20, 40, 80$. 26

Table 4.3. The computed L^2 norm of $u-u_h$ in Case 1-3 when $u(x) = (x-x^2)^2$, $p = 1, 2$, and $N = 5, 10, 20, 40, 80$. 26

Table 4.4. The computed L^2 norm of $u-u_h$ in Case 1-4 when $u(x) = (x-x^2)^2$, $p = 1, 2$, and $N = 5, 10, 20, 40, 80$. 27

Table 4.5. The computed L^2 norm of $u-u_h$ in Case 1-5 when $u(x) = (x-x^2)^2$, $p = 1, 2$, and $N = 5, 10, 20, 40, 80$. 27

Table 4.6. The computed L^2 norm of $u-u_h$ in Case 1-6 when $u(x) = (x-x^2)^2$, $p = 1, 2$, and $N = 5, 10, 20, 40, 80$. 27

Table 4.7. The computed L^2 norm of $u-u_h$ in Case 1-1 when $u(x) = \cos(\pi x)$, $p = 1, 2$, and $N = 5, 10, 20, 40, 80$. 28

Table 4.8. The computed L^2 norm of $u-u_h$ in Case 1-2 when $u(x) = \cos(\pi x)$, $p = 1, 2$, and $N = 5, 10, 20, 40, 80$. 28

Table 4.9. The computed L^2 norm of $u-u_h$ in Case 1-3 when $u(x) = \cos(\pi x)$, $p = 1, 2$, and $N = 5, 10, 20, 40, 80$. 28

Table 4.10. The computed L^2 norm of $u-u_h$ in Case 1-4 when $u(x) = \cos(\pi x)$, $p = 1, 2$, and $N = 5, 10, 20, 40, 80$. 29

Table 4.11. The computed L^2 norm of $u-u_h$ in Case 1-5 when $u(x) = \cos(\pi x)$, $p = 1, 2$, and $N = 5, 10, 20, 40, 80$. 29

Table 4.12. The computed L^2 norm of $u-u_h$ in Case 1-6 when $u(x) = \cos(\pi x)$, $p = 1, 2$, and $N = 5, 10, 20, 40, 80$. 29
Table 4.13. Convergence rates of the computed L^2 norm of $u-u_h$ in Case 1-1 when $u(x) = (x - x^2)^2$. 30
Table 4.14. Convergence rates of the computed L^2 norm of $u-u_h$ in Case 1-2 when $u(x) = (x - x^2)^2$. 30
Table 4.15. Convergence rates of the computed L^2 norm of $u-u_h$ in Case 1-3 when $u(x) = (x - x^2)^2$. 31
Table 4.16. Convergence rates of the computed L^2 norm of $u-u_h$ in Case 1-4 when $u(x) = (x - x^2)^2$. 31
Table 4.17. Convergence rates of the computed L^2 norm of $u-u_h$ in Case 1-5 when $u(x) = (x - x^2)^2$. 31
Table 4.18. Convergence rates of the computed L^2 norm of $u-u_h$ in Case 1-6 when $u(x) = (x - x^2)^2$. 32
Table 4.19. Convergence rates of the computed L^2 norm of $u-u_h$ in Case 1-1 when $u(x) = \cos(\pi x)$. 32
Table 4.20. Convergence rates of the computed L^2 norm of $u-u_h$ in Case 1-2 when $u(x) = \cos(\pi x)$. 32
Table 4.21. Convergence rates of the computed L^2 norm of $u-u_h$ in Case 1-3 when $u(x) = \cos(\pi x)$. 33
Table 4.22. Convergence rates of the computed L^2 norm of $u-u_h$ in Case 1-4 when $u(x) = \cos(\pi x)$. 33

Table 4.23. Convergence rates of the computed L^2 norm of $u - u_h$ in Case 1-5 when $u(x) = \cos(\pi x)$. 33
Table 4.24. Convergence rates of the computed L^2 norm of $u - u_h$ in Case 1-6 when $u(x) = \cos(\pi x)$. 34
Table 4.25. The computed L^2 norm of $u - u_h$ in Case 2-1: $p = 1, 2$, $u(x) = \sin(\pi x) + \pi$, $N = 5, 10, 20, 40, 80$. 43
Table 4.26. The computed L^2 norm of $u - u_h$ in Case 2-2: $p = 1, 2$, $u(x) = \sin(\pi x) + \pi$, $N = 5, 10, 20, 40, 80$. 43
Table 4.27. Convergence rates of the computed L^2 norm of $u - u_h$ in Case 2-1 when $u(x) = \sin(\pi x) + \pi$. 43
Table 4.28. Convergence rates of the computed L^2 norm of $u - u_h$ in Case 2-2 when $u(x) = \sin(\pi x) + \pi$. 44

List of Figures

Figure 4.1. The graph of $a(x)$ in (4.3). 11

Figure 4.2. The graphs of the solution $u(x) = (x-x^2)^2$ and the approximate solution u_h in Case 1-2 when $p = 1$ and $h = 0.2, 0.1, 0.05$. . . . 13

Figure 4.3. The graphs of the solution $u(x) = (x-x^2)^2$ and the approximate solution u_h in Case 1-2 when $p = 2$ and $h = 0.2, 0.1$. 14

Figure 4.4. The graphs of the solution $u(x) = (x-x^2)^2$ and the approximate solution $u_{0.1,p}$ in Case 1-2 when $p = 1, 2$. 15

Figure 4.5. The graphs of the solution $u(x) = \cos(\pi x)$ and the approximate solution u_h in Case 1-2 when $p = 1$ and $h = 0.2, 0.1, 0.05$. . . . 16

Figure 4.6. The graphs of the solution $u(x) = \cos(\pi x)$ and the approximate solution u_h in Case 1-2 when $p = 2$ and $h = 0.2, 0.1$. 17

Figure 4.7. The graphs of the solution $u(x) = \cos(\pi x)$ and the approximate solution $u_{0.2,p}$ in Case 1-2 when $p = 1, 2$. 18

Figure 4.8. The graphs of the solution $u(x) = (x-x^2)^2$ and the approximate solution u_h in Case 1-4 when $p = 1$ and $h = 0.2, 0.1, 0.05$. . . . 20

Figure 4.9. The graphs of the solution $u(x) = (x-x^2)^2$ and the approximate solution u_h in Case 1-4 when $p = 2$ and $h = 0.2, 0.1$. 21

Figure 4.10. The graphs of the solution $u(x) = (x-x^2)^2$ and the approximate solution $u_{0.1,p}$ in Case 1-4 when $p = 1, 2$. 22

Figure 4.11. The graphs of the solution $u(x) = \cos(\pi x)$ and the approximate solution u_h in Case 1-4 when $p = 1$ and $h = 0.2, 0.1, 0.05$. . 23

Figure 4.12. The graphs of the solution $u(x) = \cos(\pi x)$ and the approximate solution u_h in Case 1-4 when $p = 2$ and $h = 0.2, 0.1$. 24
Figure 4.13. The graphs of the solution $u(x) = \cos(\pi x)$ and the approximate solution $u_{0.2,p}$ in Case 1-4 when $p = 1, 2$. 25
Figure 4.14. The graphs of the solution $u(x) = \sin(\pi x) + \pi$ and the approximate solution u_h in Case 2-1 when $p = 1$ and $h = 0.2, 0.1, 0.05$. 37
Figure 4.15. The graphs of the solution $u(x) = \sin(\pi x) + \pi$ and the approximate solution u_h in Case 2-1 when $p = 2$ and $h = 0.2, 0.1$. . 38
Figure 4.16. The graphs of the solution $u(x) = \sin(\pi x) + \pi$ and the approximate solution $u_{0.1,p}$ in Case 2-1 when $p = 1, 2$. 39
Figure 4.17. The graphs of the solution $u(x) = \sin(\pi x) + \pi$ and the approximate solution u_h in Case 2-2 when $p = 1$ and $h = 0.2, 0.1, 0.05$. 40
Figure 4.18. The graphs of the solution $u(x) = \sin(\pi x) + \pi$ and the approximate solution u_h in Case 2-2 when $p = 2$ and $h = 0.2, 0.1$. . 41
Figure 4.19. The graphs of the solution $u(x) = \sin(\pi x) + \pi$ and the approximate solution $u_{0.1,p}$ in Case 2-2 when $p = 1, 2$. 42

경계값 문제에 대한 불연속 갈레르킨 방법의 수치적 연구

이청화

부경대학교 교육대학원 수학교육전공

요약

본 학위 논문에서는 과학과 공학의 여러 문제들을 설명하는 동차 혼합 경계조건을 가지는 1차원 경계값 문제에 대해서 내부 패널티를 가지는 불연속 갈레르킨 근사해의 개념을 도입하고, 다양한 경우에 있어서 근사해의 L^2노름에 대한 오차를 수치적으로 연구하였다.

1. Introduction

Discontinuous Galerkin methods with interior penalties for elliptic problems were introduced by several authors [1, 8, 15]. These methods, referred to as interior penalty Galerkin schemes but not locally mass conservative, generalized Nitche method in [11] to treat the Dirichlet boundary condition with penalty terms on the boundary of the domain.

New types of elementwise conservative discontinuous Galerkin methods for diffusion problems were introduced and a priori error estimates were analyzed in [4,9,12,13,14]. Theoretical stability analysis and optimal error estimates of all existing discontinuous Galerkin methods for elliptic problems were discussed in a unified framework in [2] and the relationship of various discontinuous finite element methods for second order elliptic equations were also discussed in [5, 6]. For a general overview and wide applications of discontinuous Galerkin methods, we refer to [7].

Recently, Babuska et al. [3] introduced a discontinuous Galerkin method for second order boundary value problems with a Dirichlet boundary condition and a Neumann boundary condition and analyzed a priori error estimates in the energy and L^2 norms. But their error estimate in the L^2 norm was not optimal. And Larson and Niklasson [10] analyzed the error in the L^2 norm of a family of discontinuous Galerkin methods, depending on two real parameters, for one dimensional elliptic problem with a Dirichlet boundary condition and a Neumann boundary condition. When $\tilde{\alpha} = -1$, the error in the L^2 norm is optimal and when $\tilde{\alpha} \neq -1$, one in the L^2 norm is optimal if

p is odd and suboptimal if p is even.

In this thesis, we consider the following boundary value problem with the mixed boundary conditions

$$-\frac{d}{dx}\Big(a(\frac{du}{dx}+bu)\Big)+du=f \quad \text{in } I=(\alpha,\beta)$$

$$\frac{du}{dx}+bu=0 \quad \text{at} \quad x=\alpha \text{ and } x=\beta$$

where a is a positive, bounded smooth function, b is a bounded smooth function, and d is a bounded nonnegative function.

The objectives of this thesis are to introduce a discontinuous Galerkin method for the boundary value problem with the mixed boundary conditions and to present the numerical results of the method - especially, the computed L^2 error of discontinuous Galerkin approximations and their convergence rates. These numerical results will give us some motivations for further theoretical studies on discontinuous Galerkin methods for the boundary value problem with the mixed boundary conditions

The outline of this thesis is organized as follows. Some notations are given in section 2 and a discontinuous weak formulation of the boundary value problem is also given in section 3. In section 4 we present some results of the numerical experiments for the problem. The main results of our numerical study are summarized in section 5.

2. Notations

Let $I = (\alpha, \beta)$ be a bounded open interval in $\mathbb{R}$ and P_h denote a partition of I, i.e., P_h a finite collection of N open subintervals $K_i = (x_{i-1}, x_i),\ \ x_{i-1} < x_i,\ \ i = 1, 2, \cdots, N$, such that

$$[\alpha, \beta] = \bigcup_{K_i \in P_h} \overline{K_i},$$
$$K_i \cap K_j = \phi, \quad i \neq j,$$

and if $h_i = x_i - x_{i-1},\ \ i = 1, 2, \cdots, N,\ \ h_{\max} = \max\{h_i\}$ and $h_{\min} = \min\{h_i\}$, then $h_{\max}/h_{\min}$ is bounded below and above by positive constants, independent of partitions P_h.

For a given partition P_h, we introduce the sets Γ and Γ_{int} as follows:

$$\Gamma = \bigcup_{K_i \in P_h} \partial K_i = \{x_0, x_1, \cdots, x_N\}$$

and

$$\Gamma_{int} = \Gamma - \partial I = \{x_1, x_2, \cdots, x_{N-1}\}$$

where $\partial K_i = \{x_{i-1}, x_i\}$ denotes the boundary of the interval K_i and $\partial I = \{x_0, x_N\}$. We define $h = h_{\max}$ and $\hat{h}_i$ as follows:

$$\hat{h}_i = \begin{cases} \frac{h_i}{2}, & x_i \in \partial K_i \cap \partial I, \\ \frac{h_i + h_{i+1}}{2}, & x_i \in (\partial K_i \cap \partial K_{i+1}) \subset \Gamma_{int}. \end{cases}$$

The unit normal vector outward from K_i is denoted by $n|_i$. For each point $x_i \in \Gamma$ we will associate a unit normal vector n. The unit normal vector n is defined as $n = -1$ if $x_i \in \Gamma_{int}$ and $n = -1$ or 1 for x_0 or x_N, respectively. Therefore,

$$n|_{i+1}(x_i) = -n|_i(x_i) = n, \quad x_i \in \Gamma_{int}$$

and

$$n|_1(x_0) = -1, \;\; n|_N(x_N) = 1.$$

Let l be a nonnegative integer. For any given open interval S (S may be the whole interval I or an element K_i of P_h), the space $H^l(S)$ will denote the usual Sobolev space with norm $\|\cdot\|_{l,S}$. The so-called (mesh-dependent) broken space $H^l(P_h)$ will be defined as

$$H^l(P_h) = \{v \in L^2(I); v|_{K_i} \in H^l(K_i), \;\; \forall K_i \in P_h\}.$$

The norm associated with the space $H^l(P_h)$ is given as

$$\|v\|_{l,h} = \Big(\sum_{K_i \in P_h} \|v\|^2_{l,K_i} \Big)^{1/2}.$$

Finite element subspaces V_h of polynomial functions will be defined as

$$V_h = \{v \in L^2(I); \;\; v|_{K_i} \in P_p(K_i), \;\; \forall K_i \in P_h\},$$

where $P_p(K_i)$ is the space of polynomial of degree less than or equal to p on K_i for a given integer $p \geq 1$.

For any function $v \in H^l(K_i) \times H^l(K_{i+1})$, $l > 1/2$, we denote the jump and average of v at $x_i \in \Gamma_{int}$, by $[v]$ and $\{v\}$, respectively, i.e.,

$$[v](x_i) = v(x_i)|_{K_{i+1}} - v(x_i)|_{K_i}, \quad x_i \in \Gamma_{int},$$
$$\{v\}(x_i) = \frac{1}{2}(v(x_i)|_{K_{i+1}} + v(x_i)|_{K_i}), \quad x_i \in \Gamma_{int}.$$

And at $x_0 and x_N$, we define

$$[v](x_0) = [v](x_N) = 0.$$

3. A Discontinuous Weak Formulation

We consider the following boundary value problem with the boundary conditions

$$-\frac{d}{dx}\Big(a(\frac{du}{dx}+bu)\Big)+du=f \quad \text{in } \ I=(\alpha,\beta) \tag{3.1}$$

$$\frac{du}{dx}+bu=0 \quad \text{at} \quad x=\alpha \ \text{and} \ x=\beta \tag{3.2}$$

where a is a positive, bounded smooth function, b is a bounded smooth function, and d is a bounded nonnegative function.

Multiplying both sides of (3.1) by v and integrating both sides, we have

$$\int_I \Big(-\frac{d}{dx}\Big(a(\frac{du}{dx}+bu)\Big)v+duv\Big)dx=\int_I fvdx. \tag{3.3}$$

And decomposing (3.3) over K_i, we obtain

$$\sum_{K_i\in P_h}\int_{K_i}-\frac{d}{dx}(a(\frac{du}{dx}+bu))vdx+\sum_{K_i\in P_h}\int_{K_i}duvdx=\sum_{K_i\in P_h}\int_{K_i}fvdx.$$

Then integration by parts gives us

$$\begin{aligned}&\sum_{K_i\in P_h}\int_{K_i}\Big(a(\frac{du}{dx}+bu)\frac{dv}{dx}+duv\Big)dx\\ &-\sum_{i=0}^{N-1}\big(na(\frac{du}{dx}+bu)v\big)|_{K_{i+1}}(x_i)-\sum_{i=1}^{N}\big(na(\frac{du}{dx}+bu)v\big)|_{K_i}(x_i)\\ &=\int_I fvdx.\end{aligned} \tag{3.4}$$

Using the formula below

$$ac-bd=\frac{1}{2}(a+b)(c-d)+\frac{1}{2}(a-b)(c+d)$$

where a, b, c and d are real numbers and using the average and jump operators, we have

$$\big(na(\frac{du}{dx}+bu)v\big)|_{K_{i+1}}(x_i)+\big(na(\frac{du}{dx}+bu)\big)|_{K_i}(x_i)$$
$$=\bigg(\Big\{na(\frac{du}{dx}+bu)\Big\}[v]+\Big[na(\frac{du}{dx}+bu)\Big]\{v\}\bigg)(x_i),$$

for a given point $x_i \in \Gamma_{int}$. Therefore, we have

$$\begin{aligned}
&\sum_{i=0}^{N-1}\big(na(\frac{du}{dx}+bu)v\big)|_{K_{i+1}}(x_i)+\sum_{i=1}^{N}\big(na(\frac{du}{dx}+bu)v\big)|_{K_i}(x_i)\\
&\quad=\sum_{i=1}^{N-1}\Big(\Big\{na(\frac{du}{dx}+bu)\Big\}[v]+\Big[na(\frac{du}{dx}+bu)\Big]\{v\}\Big)(x_i)\\
&\qquad+\Big(na(\frac{du}{dx}+bu)v\Big)(x_0)+\Big(na(\frac{du}{dx}+bu)v\Big)(x_N)\\
&\quad=\sum_{i=1}^{N-1}\Big(\Big\{na(\frac{du}{dx}+bu)\Big\}[v]\Big)(x_i),
\end{aligned}$$

because the jump of $a(\frac{du}{dx}+bu)$ is zero on Γ_{int} and $\frac{du}{dx}+bu$ is zero at ∂I. Consequently, (3.4) can now be reduced to

$$\begin{aligned}
&\sum_{K_i\in P_h}\int_{K_i}\Big(a\frac{du}{dx}\frac{dv}{dx}+abu\frac{dv}{dx}+duv\Big)dx\\
&\quad-\sum_{i=1}^{N-1}\Big(\Big\{na\frac{du}{dx}\Big\}[v]+\{nabu\}[v]\Big)(x_i)=\sum_{K_i\in P_h}\int_{K_i}fvdx.
\end{aligned}$$

Now, we introduce the following bilinear form $B(\cdot,\cdot)$ defined on $H^2(P_h)\times H^2(P_h)$ and the linear form $F(\cdot)$ defined on $H^2(P_h)$ as follows:

$$B(u,v)=\sum_{K_i\in P_h}\int_{K_i}\Big(a\frac{du}{dx}\frac{dv}{dx}+abu\frac{dv}{dx}+duv\Big)dx,$$

$$F(v) = \sum_{K_i \in P_h} \int_{K_i} fv dx = \int_I fv dx.$$

And we introduce the bilinear form $J(\cdot, \cdot)$ defined on $H^2(P_h) \times H^2(P_h)$ as follows:

$$\begin{aligned} J(u, v) &= \sum_{i=1}^{N-1} \Big(\Big\{ na \frac{du}{dx} \Big\} [v] + \{nabu\}[v] \Big)(x_i) \\ &\equiv J_1(u, v) + J_2(u, v), \quad \forall u, v \in H^2(P_h), \end{aligned}$$

where

$$J_1(u, v) = \sum_{i=1}^{N-1} \Big(\Big\{ na \frac{du}{dx} \Big\} [v] \Big)(x_i)$$

and

$$J_2(u, v) = \sum_{i=1}^{N-1} \Big(\{nabu\}[v] \Big)(x_i).$$

Thus, we define a discontinuous weak formulation of the problem (3.1) and (3.2) as follows: find $u \in H^2(P_h)$ such that

$$B(u, v) - J_1(u, v) - J_2(u, v) = F(v), \quad \forall v \in H^2(P_h).$$

Introducing the following penalty term

$$J^\sigma(u, v) = \sum_{i=0}^{N} \Big(\frac{\sigma}{\hat{h}_i} [u][v] \Big)(x_i),$$

and defining the bilinear forms $B^\sigma(\cdot, \cdot)$ on $H^2(P_h) \times H^2(P_h)$ as follows:

$$B^\sigma(u, v) = B(u, v) - J_1(u, v) - J_2(u, v) - J_1(v, u) + J^\sigma(u, v),$$

we obtain the discontinuous weak formulation of the problem (3.1) and (3.2) with an interior penalty: find $u \in H^2(P_h)$ such that

$$B^\sigma(u, v) = F(v), \quad \forall v \in H^2(P_h).$$

where σ represents a penalty parameter with $\sigma_0 = \inf_{x_i \in \Gamma_{int}} \sigma > 0$. And a discontinuous Galerkin method of the problem (3.1) and (3.2) with an interior penalty is: find $u_h \in V_h$ such that

$$B^\sigma(u_h, v) = F(v), \quad \forall v \in V_h. \tag{3.5}$$

4. Numerical Experiments

In this section, we want to present numerical results for the following boundary value problem

$$-\frac{d}{dx}\Big(a(\frac{du}{dx}+bu)\Big)+du=f, \quad \text{in } I=(0,1)$$

with the homogeneous Naumann boundary conditions

$$\frac{du}{dx}=0 \quad \text{at} \quad x=0 \text{ and } x=1 \text{ (provided that } b(0)=0 \text{ and } b(1)=0)$$

or the homogeneous mixed boundary conditions

$$\frac{du}{dx}+bu=0 \quad \text{at} \quad x=0 \text{ and } x=1 \text{ (provided that } b(0)\neq 0 \text{ and } b(1)\neq 0)$$

where a is a positive, bounded smooth function, b is a bounded smooth function, and d is a bounded nonnegative function.

4.1. Homogeneus Neumann Boundary Conditions

In this subsection, we consider the following boundary value problem with the homogeneous Neumann boundary conditions

$$-\frac{d}{dx}\Big(a(\frac{du}{dx}+bu)\Big)+du=f, \quad \text{for } I=(0,1), \tag{4.1}$$

$$\frac{du}{dx}=0 \quad \text{at} \quad x=0 \text{ and } x=1, \tag{4.2}$$

provided that $b(0)=0$ and $b(1)=0$. The function f is chosen so that the problem (4.1)-(4.2) is satisfied with the appropriate choices of $a(x)$, $b(x)$, and

$d(x)$ and the exact solution $u(x) = (x - x^2)^2$ or $\cos(\pi x)$. To perform the numerical experiments of (3.5), we consider the following six cases:

Case 1-1. $a(x) = 1$, $b(x) = 0$, and $d(x) = 1$.

Case 1-2. $a(x) = 1$, $b(x) = x(1 - x)$, and $d(x) = 1$.

Case 1-3. $a(x) = 1$, $b(x) = \sin \pi x$, and $d(x) = 1$.

Case 1-4. $b(x) = 0$, $d(x) = 1$, and $a(x)$ are given as following:

$$a(x) = \begin{cases} 9(x-0.1)^2 + 0.1, & \text{if} \quad 0 \leqslant x < 0.1, \\ 0.1, & \text{if} \quad 0.1 \leqslant x < 0.9, \\ 9(x-0.9)^2 + 0.1, & \text{if} \quad 0.9 \leqslant x \leqslant 1, \end{cases} \tag{4.3}$$

Case 1-5. $b(x) = x(1 - x)$, $d(x) = 1$, and $a(x)$ is the same as (4.3).

Case 1-6. $b(x) = \sin \pi x$, $d(x) = 1$, and $a(x)$ is the same as (4.3).

The graph of $a(x)$ in (4.3) are given in Figure 4.1.

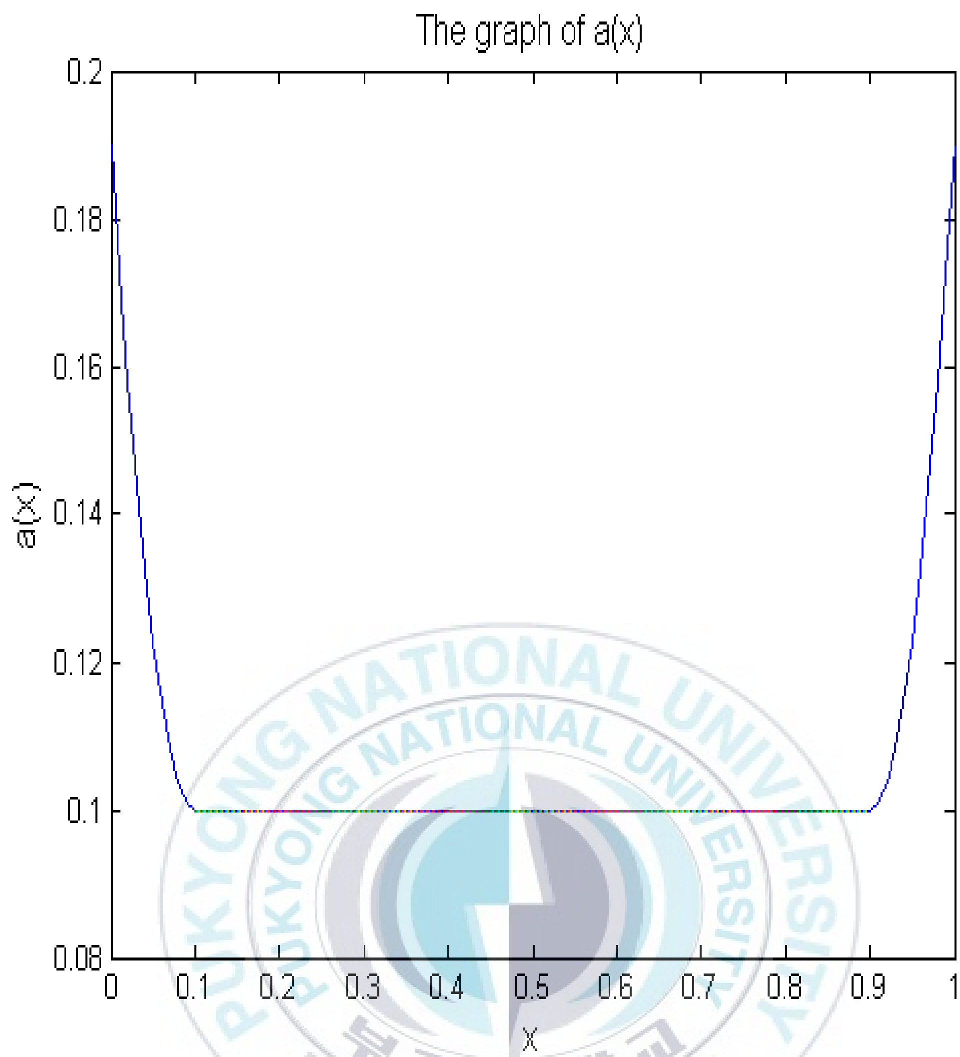

Figure 4.1. The graph of $a(x)$ in (4.3).

To implement the discontinuous Galerkin method (3.5)

$$B^{\sigma}(u_h, v) = F(v), \quad \forall v \in V_h,$$

we take P_h as the collection of N uniform subintervals in I with its length $h = 1/N$ and

$$V_h = \{v \in L^2(I);\ v|_{K_i} \in P_p(K_i),\ \forall K_i \in P_h\},$$

as the finite dimensional subspace of $H^2(P_h)$ where $p \geqslant 1$.

In Figure 4.2 and Figure 4.3(or in Figure 4.5 and Figure 4.6), we plot the exact solution $u = (x - x^2)^2$(or $u = \cos(\pi x)$, respectively) and the approximate solution u_h of (3.5) with different values of h for Case 1-2 when $p = 1$ and $p = 2$, respectively. We know from Figure 4.2 and Figure 4.3(or from Figure 4.5 and Figure 4.6) that the approximate solution u_h converges to the exact solution $u = (x - x^2)^2$(or $u = \cos(\pi x)$, respectively) as the size of h decreases.

In Figure 4.4, we plot the exact solution $u = (x-x^2)^2$ and the approximate solution $u_{0.1,p}$ of (3.5) with $p = 1, 2$ for Case 1-2 when $h = 0.1$. We know from Figure 4.4 that the approximate solution $u_{0.1,2}$ is more close to the exact solution $u = (x - x^2)^2$ than the approximate solution $u_{0.1,1}$. In Figure 4.7, we plot the exact solution $u = \cos(\pi x)$ and the approximate solution $u_{0.2,p}$ of (3.5) with $p = 1, 2$ for Case 1-2 when $h = 0.2$. We know from Figure 4.7 that the approximate solution $u_{0.2,2}$ is more close to the exact solution $u = \cos(\pi x)$ than the approximate solution $u_{0.2,1}$

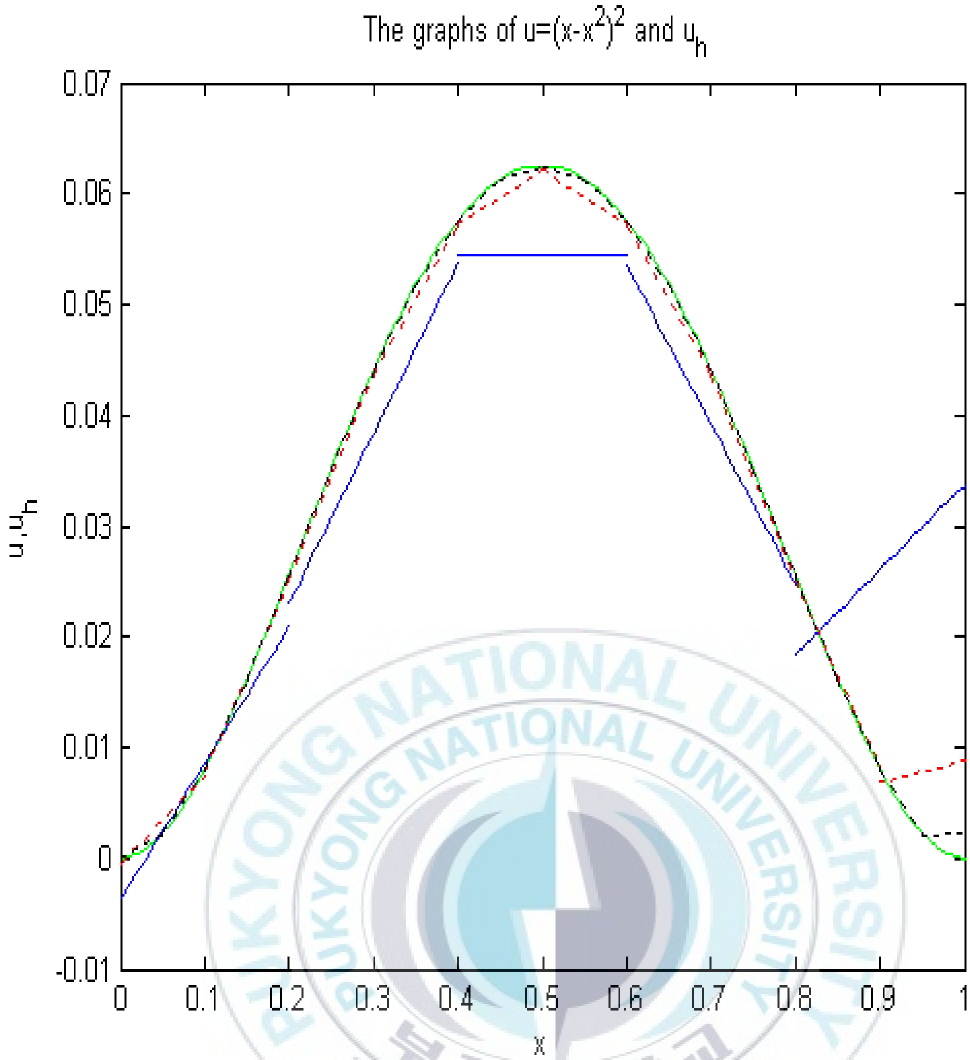

Figure 4.2. The graphs of the solution $u(x) = (x - x^2)^2$ and the approximate solution u_h in Case 1-2 when $p = 1$ and $h = 0.2, 0.1, 0.05$. The solid green line (the solution u), the solid blue line ($u_{0.2}$), the dotted red line ($u_{0.1}$), the dotted black line ($u_{0.05}$).

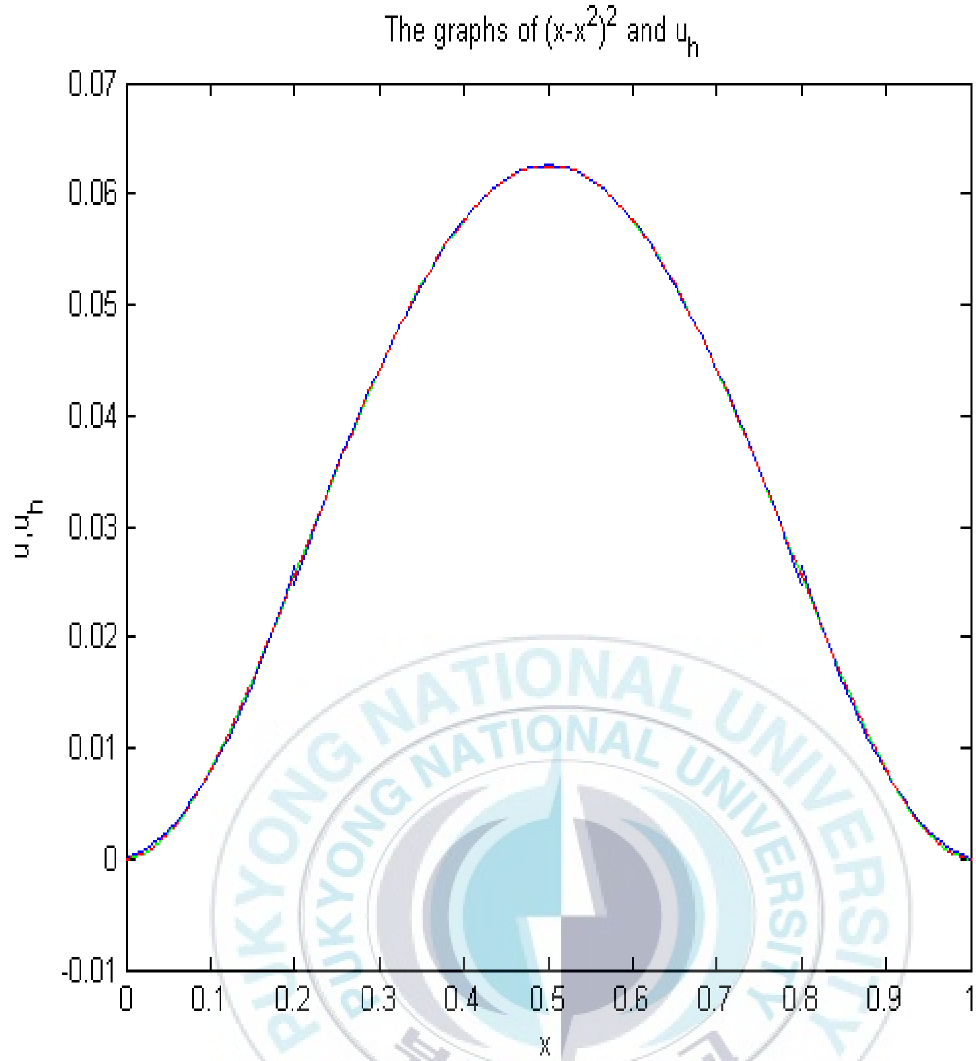

Figure 4.3. The graphs of the solution $u(x) = (x - x^2)^2$ and the approximate solution u_h in Case 1-2 when $p = 2$ and $h = 0.2, 0.1$. The solid green line (the solution u), the solid blue line ($u_{0.2}$), the dotted red line ($u_{0.1}$).

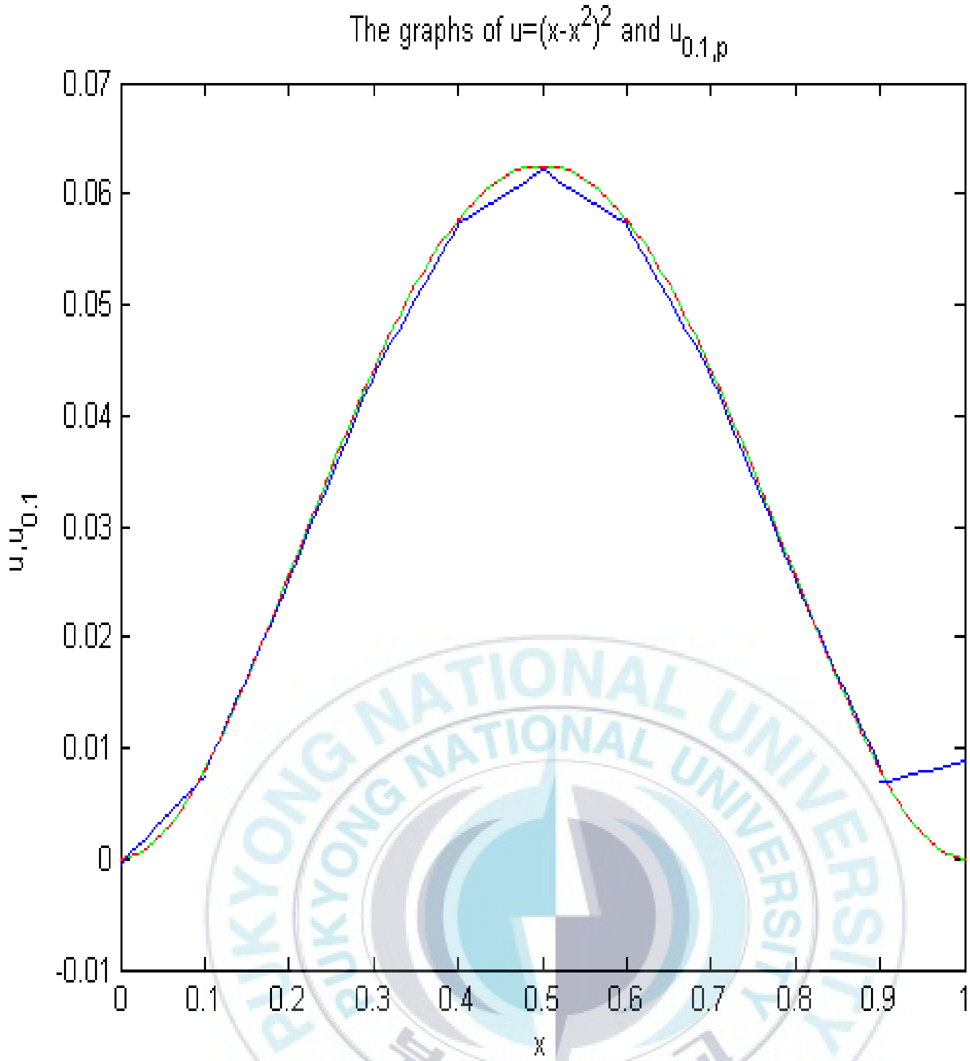

Figure 4.4. The graphs of the solution $u(x) = (x - x^2)^2$ and the approximate solution $u_{0.1,p}$ in Case 1-2 when $p = 1, 2$. The solid green line (the solution u), the solid blue line ($u_{0.1,1}$), the dotted red line ($u_{0.1,2}$).

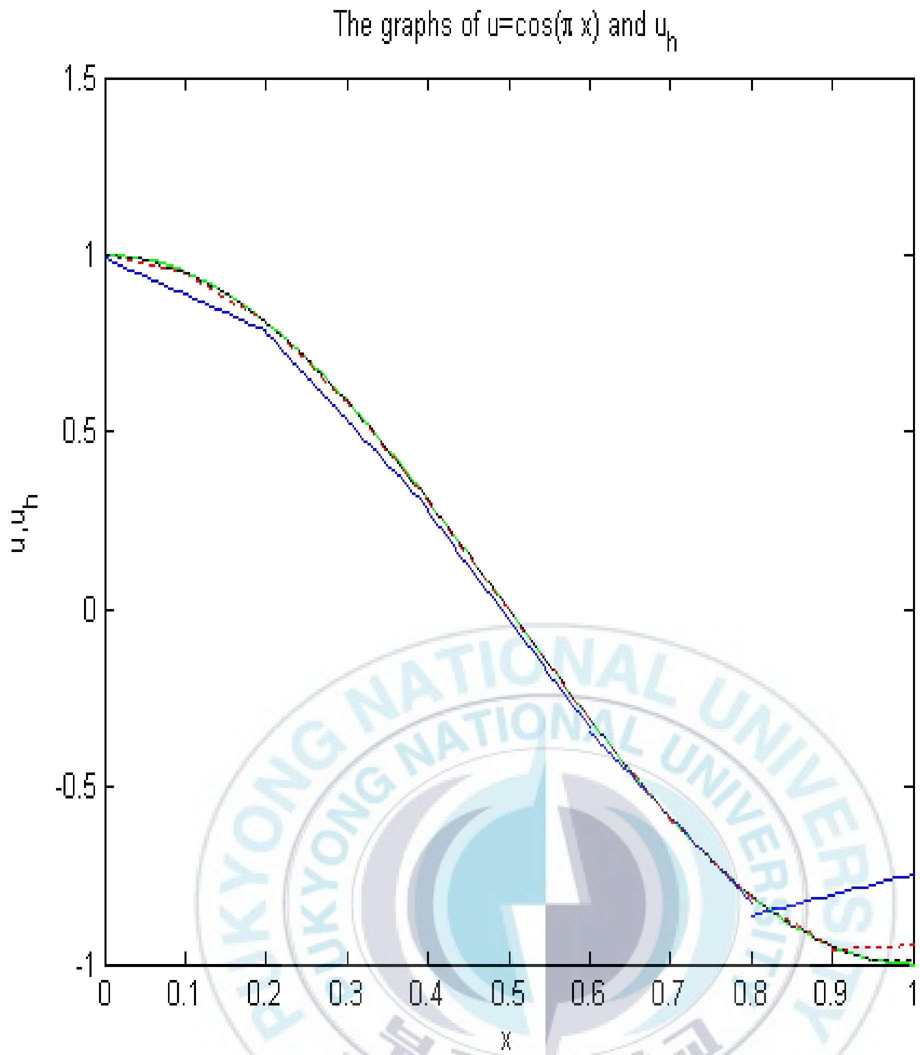

Figure 4.5. The graphs of the solution $u(x) = \cos(\pi x)$ and the approximate solution u_h in Case 1-2 when $p = 1$ and $h = 0.2, 0.1, 0.05$. The solid green line (the solution u), the solid blue line ($u_{0.2}$), the dotted red line ($u_{0.1}$), the dotted black line ($u_{0.05}$).

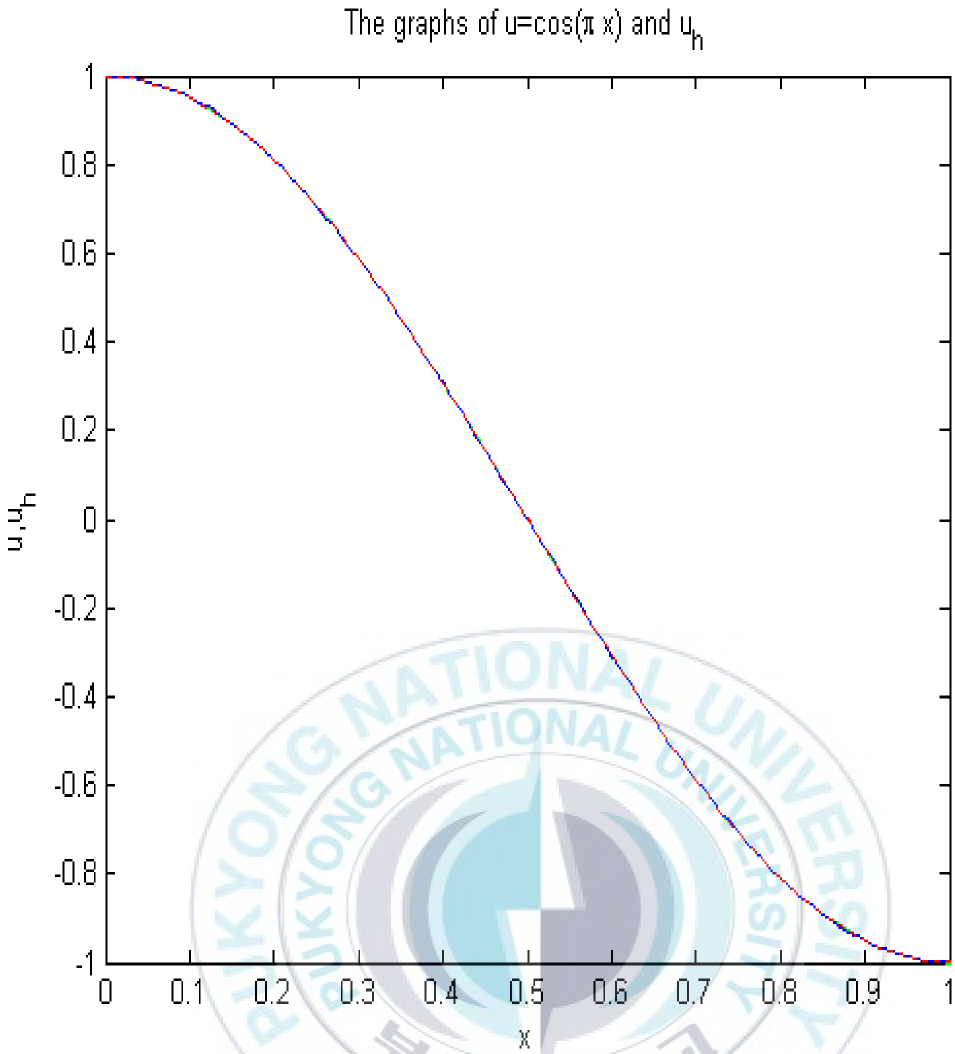

Figure 4.6. The graphs of the solution $u(x) = \cos(\pi x)$ and the approximate solution u_h in Case 1-2 when $p = 2$ and $h = 0.2, 0.1$. The solid green line (the solution u), the solid blue line ($u_{0.2}$), the dotted red line ($u_{0.1}$).

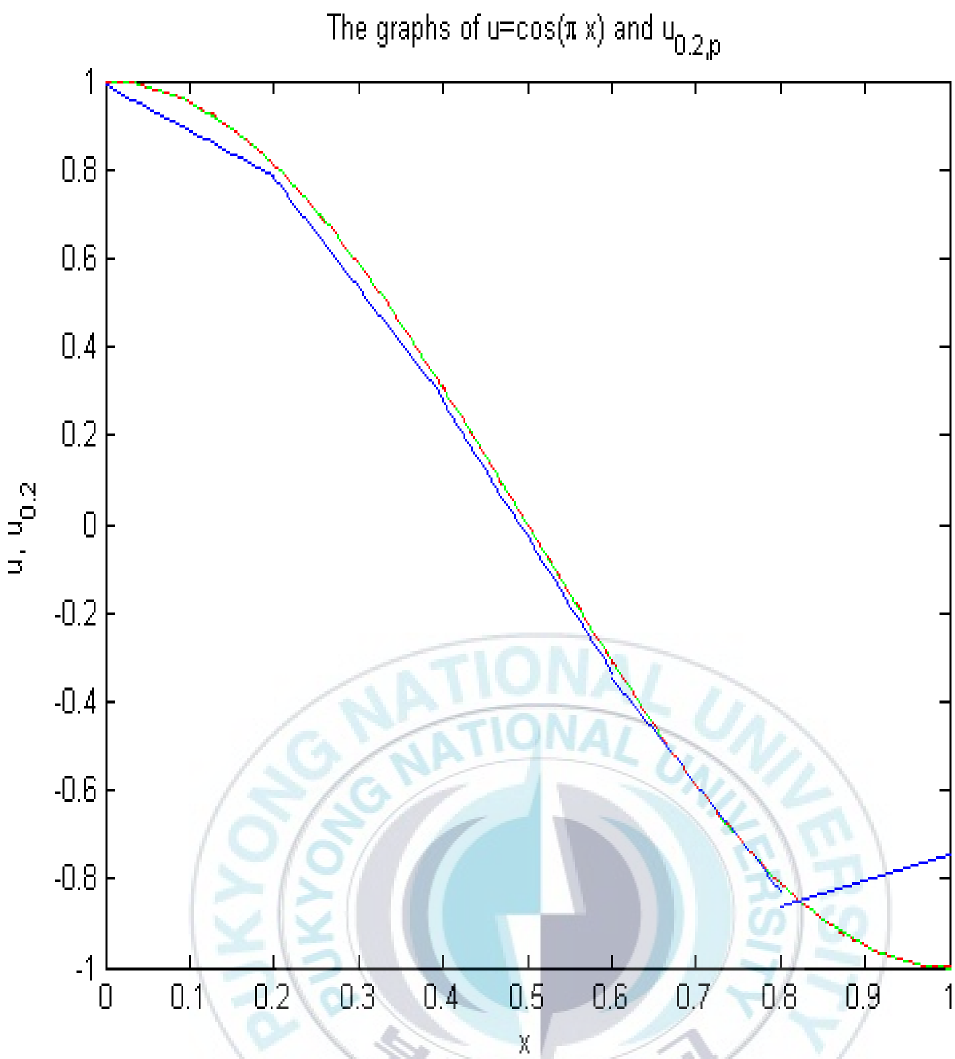

Figure 4.7. The graphs of the solution $u(x) = \cos(\pi x)$ and the approximate solution $u_{0.2,p}$ in Case 1-2 when $p = 1, 2$. The solid green line (the solution u), the solid blue line ($u_{0.2,1}$), the dotted red line ($u_{0.2,2}$).

In Figure 4.8 and Figure 4.9 (or in Figure 4.11 and Figure 4.12), we plot the exact solution $u = (x - x^2)^2$(or $u = \cos(\pi x)$, respectively) and the approximate solution u_h of (3.5) with different values of h for Case 1-4 when $p = 1$ and $p = 2$, respectively. We know from Figure 4.8 and Figure 4.9(or from Figure 4.11 and Figure 4.12) that the approximate solution u_h converges to the exact solution $u = (x - x^2)^2$(or $u = \cos(\pi x)$, respectively) as the size of h decreases.

In Figure 4.10, we plot the exact solution $u = (x - x^2)^2$ and the approximate solution $u_{0.1,p}$ of (3.5) with $p = 1, 2$ for Case 1-4 when $h = 0.1$. We know from Figure 4.10 that the approximate solution $u_{0.1,2}$ is more close to the exact solution $u = (x - x^2)^2$ than the approximate solution $u_{0.1,1}$. In Figure 4.13, we plot the exact solution $u = \cos(\pi x)$ and the approximate solution $u_{0.2,p}$ of (3.5) with $p = 1, 2$ for Case 1-4 when $h = 0.2$. We know from Figure 4.13 that the approximate solution $u_{0.2,2}$ is more close to the exact solution $u = \cos(\pi x)$ than the approximate solution $u_{0.2,1}$

In Tables 4.1-4.6(or in Tables 4.7-4.12), we present the computed L^2 norm of $u - u_h$ in Cases 1-1, 1-2, 1-3, 1-4, 1-5, and 1-6 when the discontinuous Galerkin method (3.5) is used to approximate the exact solution $u(x) = (x - x^2)^2$(or $u = \cos(\pi x)$, respectively) for $p = 1, 2$ and $N = 5, 10, 20, 40, 80$. We know from Tables 4.1-4.6(or in Tables 4.7-4.12) that the computed L^2 norm of $u - u_h$ decreases as the size of h decreases.

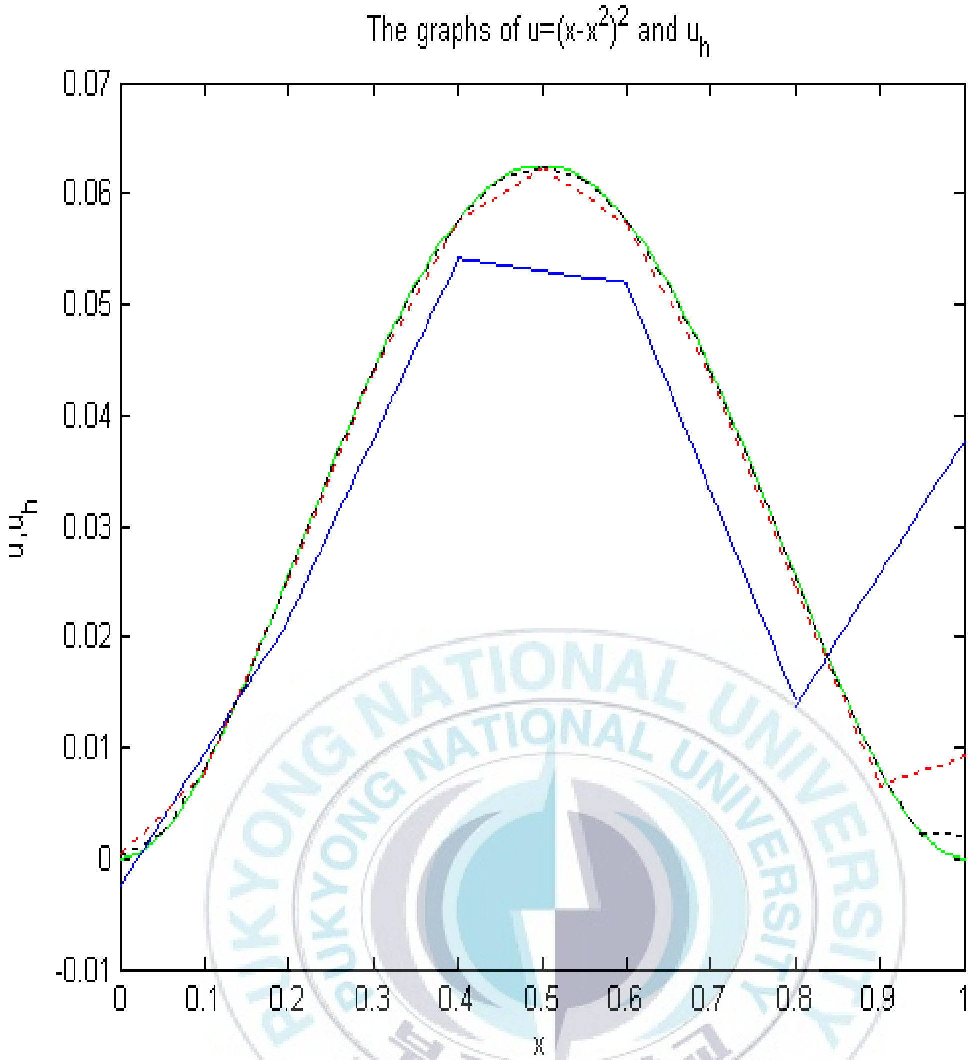

Figure 4.8. The graphs of the solution $u(x) = (x - x^2)^2$ and the approximate solution u_h in Case 1-4 when $p = 1$ and $h = 0.2, 0.1, 0.05$. The solid green line (the solution u), the solid blue line ($u_{0.2}$), the dotted red line ($u_{0.1}$), the dotted black line ($u_{0.05}$).

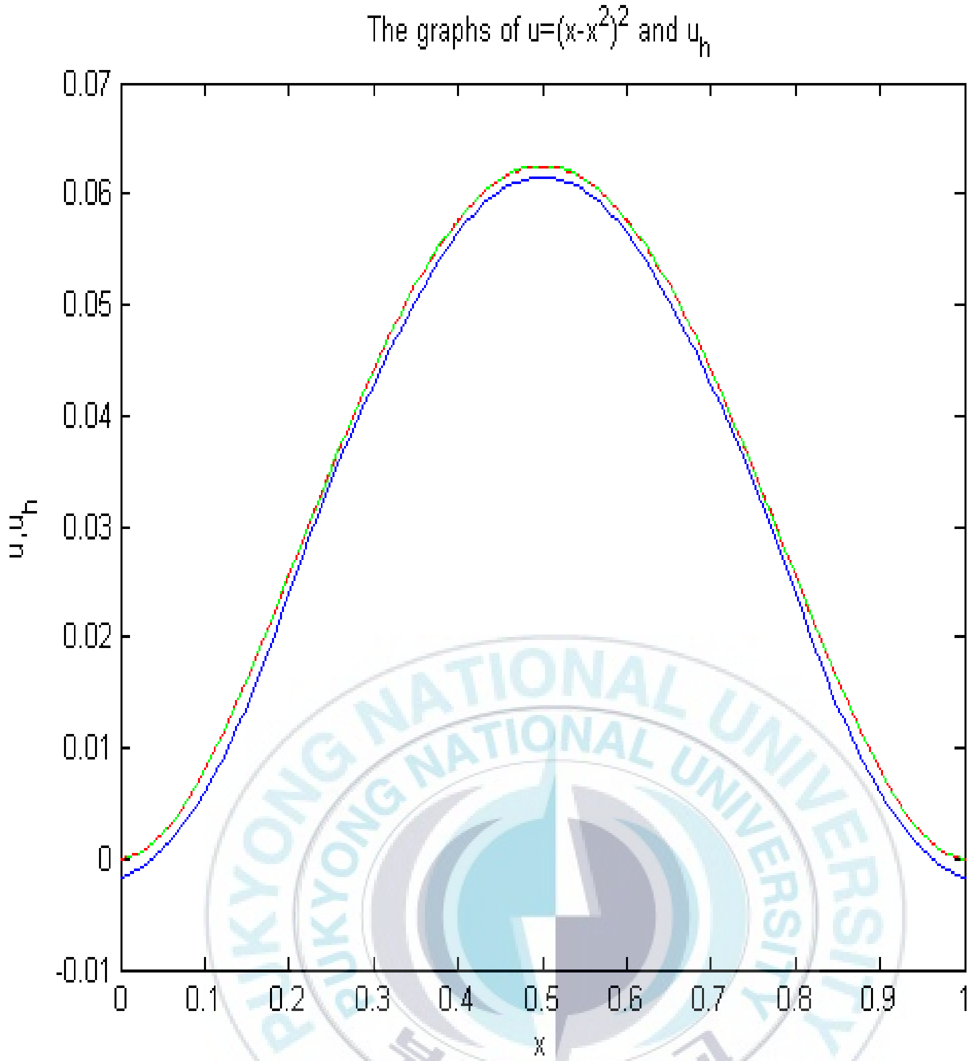

Figure 4.9. The graphs of the solution $u(x) = (x - x^2)^2$ and the approximate solution u_h in Case 1-4 when $p = 2$ and $h = 0.2, 0.1$. The solid green line (the solution u), the solid blue line ($u_{0.2}$), the dotted red line ($u_{0.1}$).

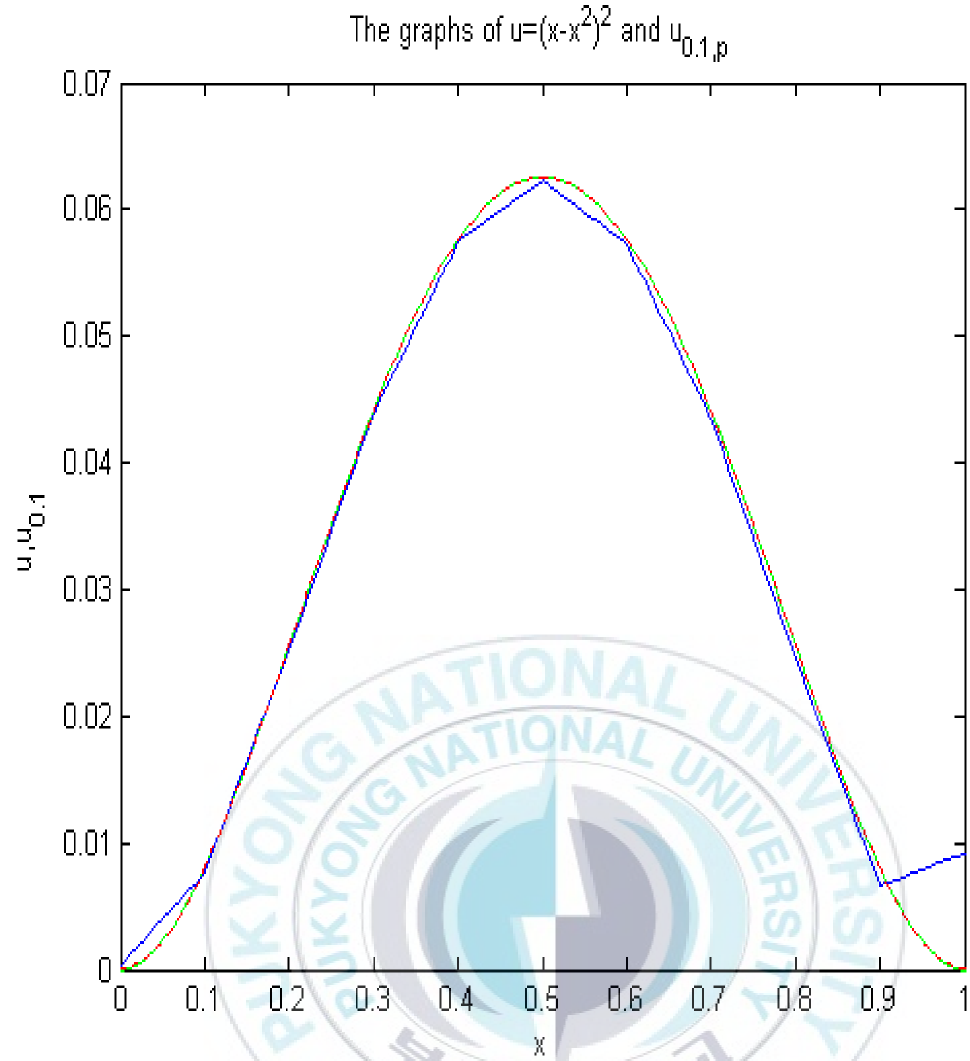

Figure 4.10. The graphs of the solution $u(x) = (x - x^2)^2$ and the approximate solution $u_{0.1,p}$ in Case 1-4 when $p = 1, 2$. The solid green line (the solution u), the solid blue line ($u_{0.1,1}$), the dotted red line ($u_{0.1,2}$).

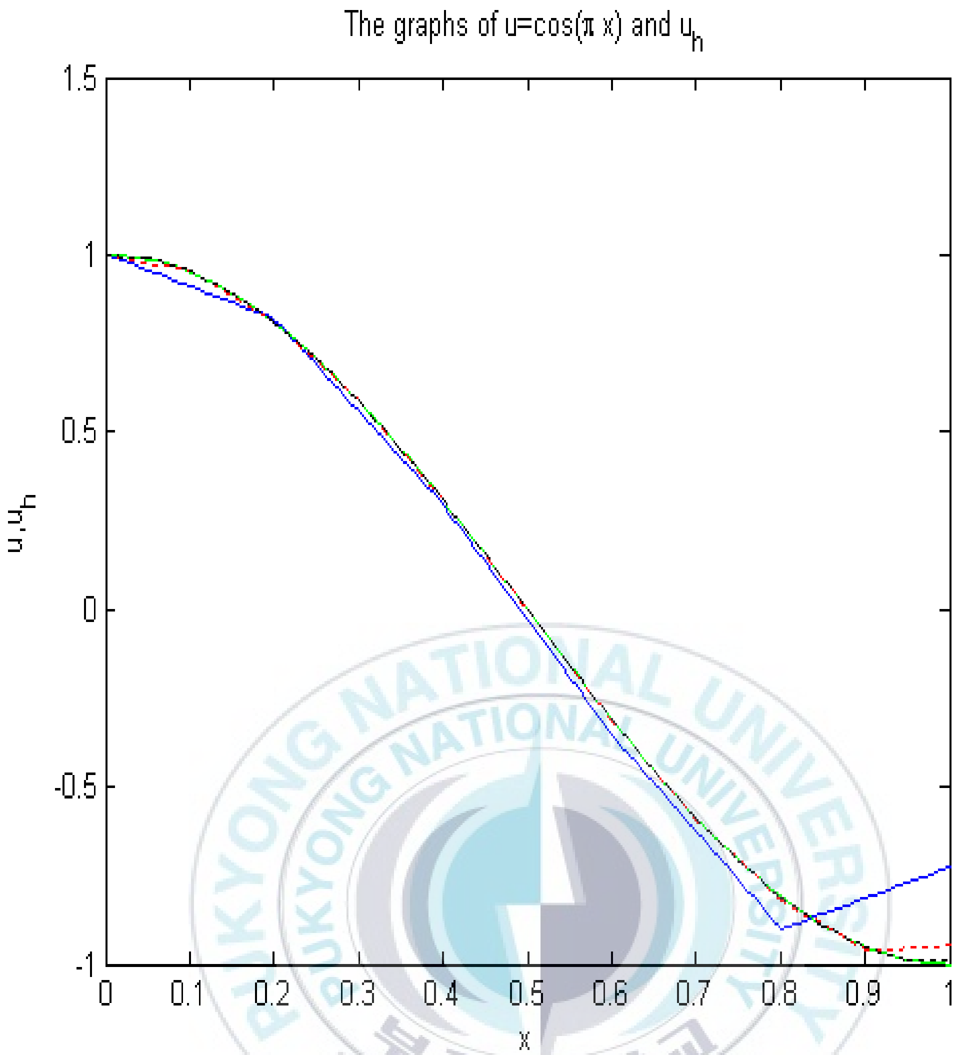

Figure 4.11. The graphs of the solution $u(x) = \cos(\pi x)$ and the approximate solution u_h in Case 1-4 when $p = 1$ and $h = 0.2, 0.1, 0.05$. The solid green line (the solution u), the solid blue line ($u_{0.2}$), the dotted red line ($u_{0.1}$), the dotted black line ($u_{0.05}$).

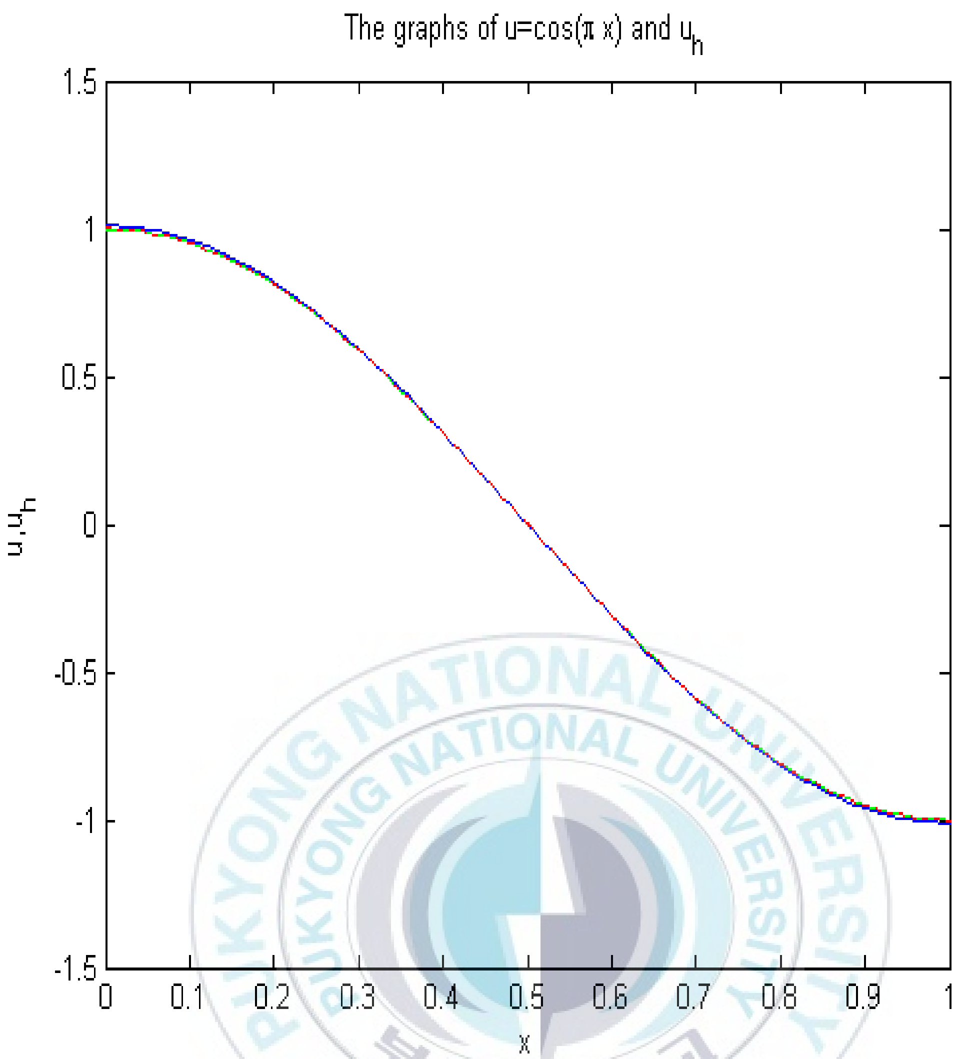

Figure 4.12. he graphs of the solution $u(x) = \cos(\pi x)$ and the approximate solution u_h in Case 1-4 when $p = 2$ and $h = 0.2, 0.1$. The solid green line (the solution u), the solid blue line ($u_{0.2}$), the dotted red line ($u_{0.1}$).

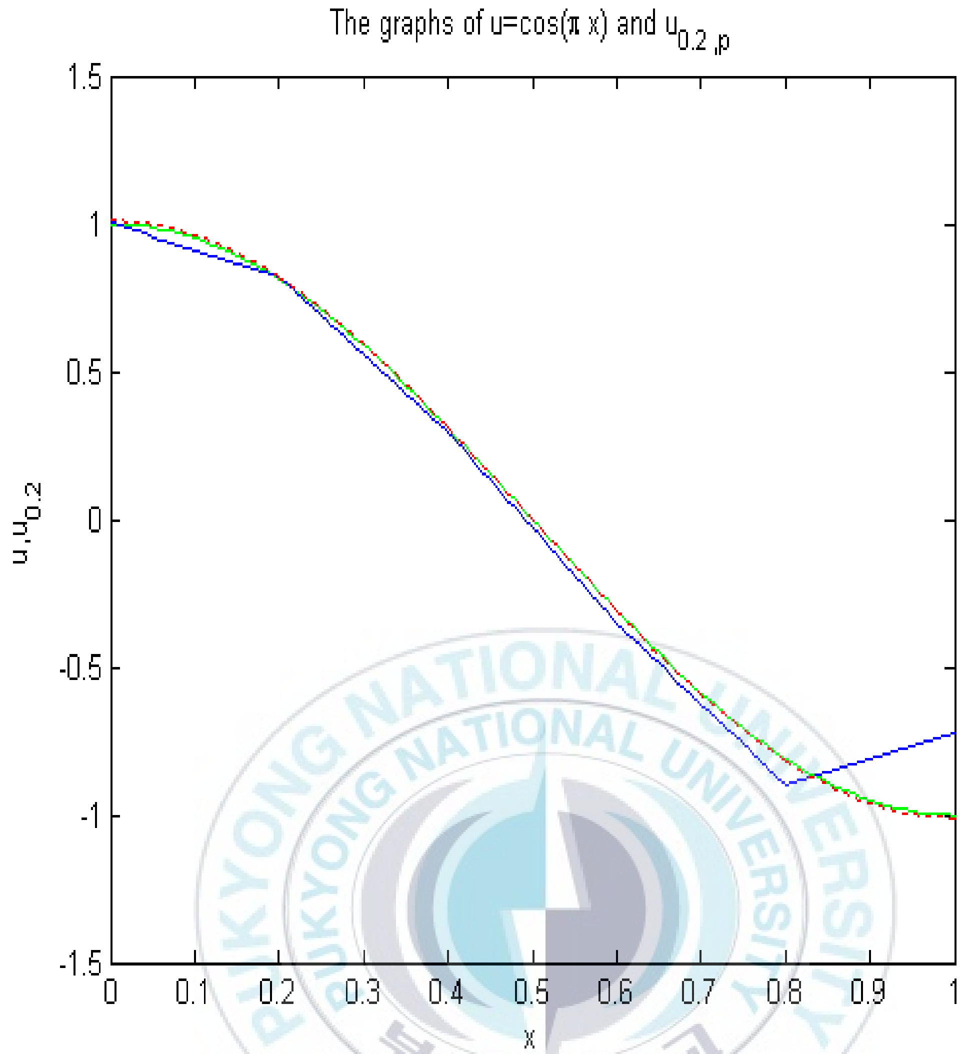

Figure 4.13. The graphs of the solution $u(x) = \cos(\pi x)$ and the approximate solution $u_{0.2,p}$ in Case 1-4 when $p = 1, 2$. The solid green line (the solution u), the solid blue line ($u_{0.2,1}$), the dotted red line ($u_{0.2,2}$).

Table 4.1. The computed L^2 norm of $u-u_h$ in Case 1-1 when $u(x) = (x-x^2)^2$, $p = 1, 2,$ and $N = 5, 10, 20, 40, 80$.

N	p=1	p=2
5	9.953610087696579E-003	2.474883001083669E-004
10	1.996926760365519E-003	2.788361382458024E-005
20	3.985452619237015E-004	3.230876615689099E-006
40	8.049477747141389E-005	3.854248624324413E-007
80	1.688806627370424E-005	4.693422770262065E-008

Table 4.2. The computed L^2 norm of $u-u_h$ in Case 1-2 when $u(x) = (x-x^2)^2$, $p = 1, 2,$ and $N = 5, 10, 20, 40, 80$.

N	p=1	p=2
5	1.008759853006282E-002	2.474876354671905E-004
10	2.009883017787915E-003	2.788359792118674E-005
20	3.999603469688148E-004	3.230876252946803E-006
40	8.066290664956095E-005	3.854248521377996E-007
80	1.690871900584171E-005	4.693422739587137E-008

Table 4.3. The computed L^2 norm of $u-u_h$ in Case 1-3 when $u(x) = (x-x^2)^2$, $p = 1, 2,$ and $N = 5, 10, 20, 40, 80$.

N	p=1	p=2
5	1.047758966574634E-002	2.474781830465663E-004
10	2.046443497883973E-003	2.788342483102578E-005
20	4.039021089603619E-004	3.230872572321048E-006
40	8.111214647928727E-005	3.854247492646964E-007
80	1.695718883572350E-005	4.693422423783653E-008

Table 4.4. The computed L^2 norm of $u-u_h$ in Case 1-4 when $u(x) = (x-x^2)^2$, $p = 1, 2,$ and $N = 5, 10, 20, 40, 80.$

N	p=1	p=2
5	1.160035209043823E-002	1.530525067065913E-003
10	2.086408645031970E-003	3.883212118173793E-005
20	4.070988201503124E-004	4.687778454455222E-006
40	8.258434258019848E-005	5.782568858044225E-007
80	1.726725774412796E-005	7.185920782352317E-008

Table 4.5. The computed L^2 norm of $u-u_h$ in Case 1-5 when $u(x) = (x-x^2)^2$, $p = 1, 2,$ and $N = 5, 10, 20, 40, 80.$

N	p=1	p=2
5	1.171286284826308E-002	1.531193383114409E-003
10	2.093441680547620E-003	3.883214671299329E-005
20	4.077089964103946E-004	4.687779172060500E-006
40	8.264633906571690E-005	5.782569068722837E-007
80	1.727387934991122E-005	7.185920841606181E-008

Table 4.6. The computed L^2 norm of $u-u_h$ in Case 1-6 when $u(x) = (x-x^2)^2$, $p = 1, 2,$ and $N = 5, 10, 20, 40, 80.$

N	p=1	p=2
5	1.203533820175762E-002	1.540061232552839E-003
10	2.111563333979656E-003	3.883246536713067E-005
20	4.091709449596473E-004	4.687788281918771E-006
40	8.276911139676766E-005	5.782571767266118E-007
80	1.727933541315180E-005	7.185921662812752E-008

Table 4.7. The computed L^2 norm of $u - u_h$ in Case 1-1 when $u(x) = \cos(\pi x)$, $p = 1, 2,$ and $N = 5, 10, 20, 40, 80$.

N	p=1	p=2
5	7.853369062906306E-002	6.191721695028490E-004
10	1.277632758534509E-002	7.480029694394360E-005
20	2.389065194578182E-003	9.267642213583770E-006
40	4.895849362524466E-004	1.155870694472144E-006
80	1.078315442788144E-004	1.444029921092537E-007

Table 4.8. The computed L^2 norm of $u - u_h$ in Case 1-2 when $u(x) = \cos(\pi x)$, $p = 1, 2,$ and $N = 5, 10, 20, 40, 80$.

N	p=1	p=2
5	7.871944593592956E-002	6.191701436555256E-004
10	1.272098979378700E-002	7.480021263942763E-005
20	2.376641402721869E-003	9.267639419728970E-006
40	4.875145782297269E-004	1.155870605388768E-006
80	1.075162369734709E-004	1.444029898124735E-007

Table 4.9. The computed L^2 norm of $u - u_h$ in Case 1-3 when $u(x) = \cos(\pi x)$, $p = 1, 2,$ and $N = 5, 10, 20, 40, 80$.

N	p=1	p=2
5	8.006365752057222E-002	6.191417005480168E-004
10	1.279858374297926E-002	7.479900893029372E-005
20	2.383660444324945E-003	9.267599428851199E-006
40	4.877449205107439E-004	1.155869337289699E-006
80	1.073231585596627E-004	1.444029499832295E-007

Table 4.10. The computed L^2 norm of $u - u_h$ in Case 1-4 when $u(x) = \cos(\pi x)$, $p = 1, 2$, and $N = 5, 10, 20, 40, 80$.

N	p=1	p=2
5	7.834650733441401E-002	6.685725516488358E-003
10	1.158396867628605E-002	1.171001827487290E-004
20	2.088796340979553E-003	1.464711764342016E-005
40	4.146895611995628E-004	1.831291118230662E-006
80	8.718656287071192E-005	2.289245803782336E-007

Table 4.11. The computed L^2 norm of $u - u_h$ in Case 1-5 when $u(x) = \cos(\pi x)$, $p = 1, 2$, and $N = 5, 10, 20, 40, 80$.

N	p=1	p=2
5	7.887411184553758E-002	6.720183895275394E-003
10	1.156238352382213E-002	1.171003936604371E-004
20	2.079586599955892E-003	1.464712441202760E-005
40	4.126296014714767E-004	1.831291334325205E-006
80	8.682852248043320E-005	2.289245839405780E-007

Table 4.12. The computed L^2 norm of $u - u_h$ in Case 1-6 when $u(x) = \cos(\pi x)$, $p = 1, 2$, and $N = 5, 10, 20, 40, 80$.

N	p=1	p=2
5	8.087740920742839E-002	7.051855680467116E-003
10	1.162402333707581E-002	1.171034347214642E-004
20	2.082891216358673E-003	1.464722162508282E-005
40	4.129869475281320E-004	1.831294387358310E-006
80	8.687126689651546E-005	2.289246792473843E-007

To get the numerical convergence rate of the computed L^2 norm of $u-u_h$, we define CR_h by

$$CR_h = \frac{\log(||u-u_h||/||u-u_{h/2}||)}{\log 2}.$$

Using the values in Tables 4.1-4.12, we obtain the values of CR_h in Tables 4.13-4.24. We know from Tables 4.13-4.24 that the numerical convergence rates of the computed L^2 norm of $u-u_h$ are $O(h^{p+1})$, where p denotes the degree of polynomials in V_h. Notice that these results are not proved theoretically.

Table 4.13. Convergence rates of the computed L^2 norm of $u-u_h$ in Case 1-1 when $u(x)=(x-x^2)^2$.

N	p=1	p=2
5	2.32	3.15
10	2.33	3.11
20	2.31	3.07
40	2.25	3.04

Table 4.14. Convergence rates of the computed L^2 norm of $u-u_h$ in Case 1-2 when $u(x)=(x-x^2)^2$.

N	p=1	p=2
5	2.33	3.05
10	2.32	3.01
20	2.31	3.00
40	2.25	3.00

Table 4.15. Convergence rates of the computed L^2 norm of $u - u_h$ in Case 1-3 when $u(x) = (x - x^2)^2$.

N	p=1	p=2
5	2.36	3.15
10	2.34	3.11
20	2.32	3.07
40	2.26	3.04

Table 4.16. Convergence rates of the computed L^2 norm of $u - u_h$ in Case 1-4 when $u(x) = (x - x^2)^2$.

N	p=1	p=2
5	2.48	5.30
10	2.36	3.05
20	2.30	3.02
40	2.26	3.01

Table 4.17. Convergence rates of the computed L^2 norm of $u - u_h$ in Case 1-5 when $u(x) = (x - x^2)^2$.

N	p=1	p=2
5	2.48	5.30
10	2.36	3.05
20	2.30	3.02
40	2.26	3.01

Table 4.18. Convergence rates of the computed L^2 norm of $u - u_h$ in Case 1-6 when $u(x) = (x - x^2)^2$.

N	p=1	p=2
5	2.51	5.31
10	2.37	3.05
20	2.31	3.02
40	2.26	3.01

Table 4.19. Convergence rates of the computed L^2 norm of $u - u_h$ in Case 1-1 when $u(x) = \cos(\pi x)$.

N	p=1	p=2
5	2.62	3.05
10	2.42	3.01
20	2.29	3.00
40	2.18	3.00

Table 4.20. Convergence rates of the computed L^2 norm of $u - u_h$ in Case 1-2 when $u(x) = \cos(\pi x)$.

N	p=1	p=2
5	2.63	3.05
10	2.42	3.01
20	2.29	3.00
40	2.18	3.00

Table 4.21. Convergence rates of the computed L^2 norm of $u - u_h$ in Case 1-3 when $u(x) = \cos(\pi x)$.

N	p=1	p=2
5	2.65	3.05
10	2.43	3.01
20	2.29	3.00
40	2.18	3.00

Table 4.22. Convergence rates of the computed L^2 norm of $u - u_h$ in Case 1-4 when $u(x) = \cos(\pi x)$.

N	p=1	p=2
5	2.76	5.84
10	2.47	3.00
20	2.33	3.00
40	2.25	3.00

Table 4.23. Convergence rates of the computed L^2 norm of $u - u_h$ in Case 1-5 when $u(x) = \cos(\pi x)$.

N	p=1	p=2
5	2.77	5.84
10	2.48	2.99
20	2.33	2.99
40	2.25	3.00

Table 4.24. Convergence rates of the computed L^2 norm of $u - u_h$ in Case 1-6 when $u(x) = \cos(\pi x)$.

N	p=1	p=2
5	2.80	5.91
10	2.48	3.00
20	2.33	3.00
40	2.25	3.00

4.2. Homogeneus Mixed Boundary Conditions

In this subsection, we consider the following boundary value problem with homogeneous mixed boundary condtions

$$-\frac{d}{dx}\Big(a(\frac{du}{dx} + bu)\Big) + du = f \quad \text{for } I = (0,1), \tag{4.4}$$

$$\frac{du}{dx} + bu = 0 \quad \text{at} \quad x = 0 \text{ and } x = 1, \tag{4.5}$$

provided that $b(0) \neq 0$ and $b(1) \neq 0$. The function f is chosen so that the problem (4.4)-(4.5) is satisfied with the appropriate choices of $a(x)$, $b(x)$, and $d(x)$ and the exact solution $u(x) = \sin(\pi x) + \pi$.

To perform the numerical experiments of (3.5), we consider the following two cases:

Case 2-1. $a(x) = 1$, $b(x) = 2(x - 1/2)$ and $d(x) = 1$,

Case 2-2. $a(x)$ is the same as (4.3), $b(x) = 2(x - 1/2)$ and $d(x) = 1$.

To implement the discontinuous Galerkin method (3.5)

$$B^\sigma(u_h, v) = F(v), \quad \forall v \in V_h,$$

we take P_h as the collection of N uniform subintervals in I with its length $h = 1/N$ and

$$V_h = \{v \in L^2(I);\ \ v|_{K_i} \in P_p(K_i),\ \ \forall K_i \in P_h\},$$

as the finite dimensional subspace of $H^2(P_h)$ where $p \geqslant 1$.

We plot the exact solution $u = \sin(\pi x) + \pi$ and the approximate solution u_h of (3.5) in Figure 4.14 and Figure 4.15 for Case 2-1 with different values of h when $p = 1$ and $p = 2$, respectively. We know from Figure 4.14 and Figure 4.15 that the approximate solution u_h converges to the exact solution $u = \sin(\pi x) + \pi$ as the size of h decreases. And in Figure 4.16, we plot the exact solution $u = \sin(\pi x) + \pi$ and the approximate solution $u_{0.1,p}$ of (3.5) with $p = 1, 2$ for Case 2-1 when $h = 0.1$. We know from Figure 4.16 that the approximate solution $u_{0.1,2}$ is more close to the exact solution $u = \sin(\pi x)+\pi$ than the approximate solution $u_{0.1,1}$.

In Figure 4.17 and Figure 4.18, we plot the exact solution $u = \sin(\pi x) + \pi$ and the approximate solution u_h of (3.5) with different values of h for Case 2-2 when $p = 1$ and $p = 2$, respectively. We know from Figure 4.17 and Figure 4.18 that the approximate solution u_h converges to the exact solution $u = \sin(\pi x) + \pi$ as the size of h decreases. And in Figure 4.19, we plot the exact solution $u = \sin(\pi x) + \pi$ and the approximate solution $u_{0.1,p}$ of (3.5) with $p = 1, 2$ for Case 2-2 when $h = 0.1$. We know from Figure 4.19 that the approximate solution $u_{0.1,2}$ is more close to the exact solution $u = \sin(\pi x)+\pi$ than the approximate solution $u_{0.1,1}$.

In Tables 4.25-4.26, we present the computed L^2 norm of $u - u_h$ in

Cases 2-1 and 2-2 when the discontinuous Galerkin method (3.5) is used to approximate the exact solution $u(x) = \sin(\pi x) + \pi$ for $p = 1, 2$ and $N = 5, 10, 20, 40, 80$. We know from Tables 4.25-4.26 that the computed L^2 norm of $u - u_h$ decrease as the size of h decreases. We have some difficulty in obtaining the approximate solution u_h in Case 2-2 with $p = 1$ and $N = 80$.

Using the values in Tables 4.25-4.26, we obtain the values of CR_h in Tables 4.27-4.28. We know from Tables 4.27-4.28 that the numerical convergence rates of the computed L^2 norm of $u - u_h$ are

$$O(h^{3/2}) \text{ when } p = 1 \quad \text{and} \quad O(h^3) \text{ when } p = 2$$

where p denotes the degree of polynomials in V_h. Notice that these results are not proved theoretically.

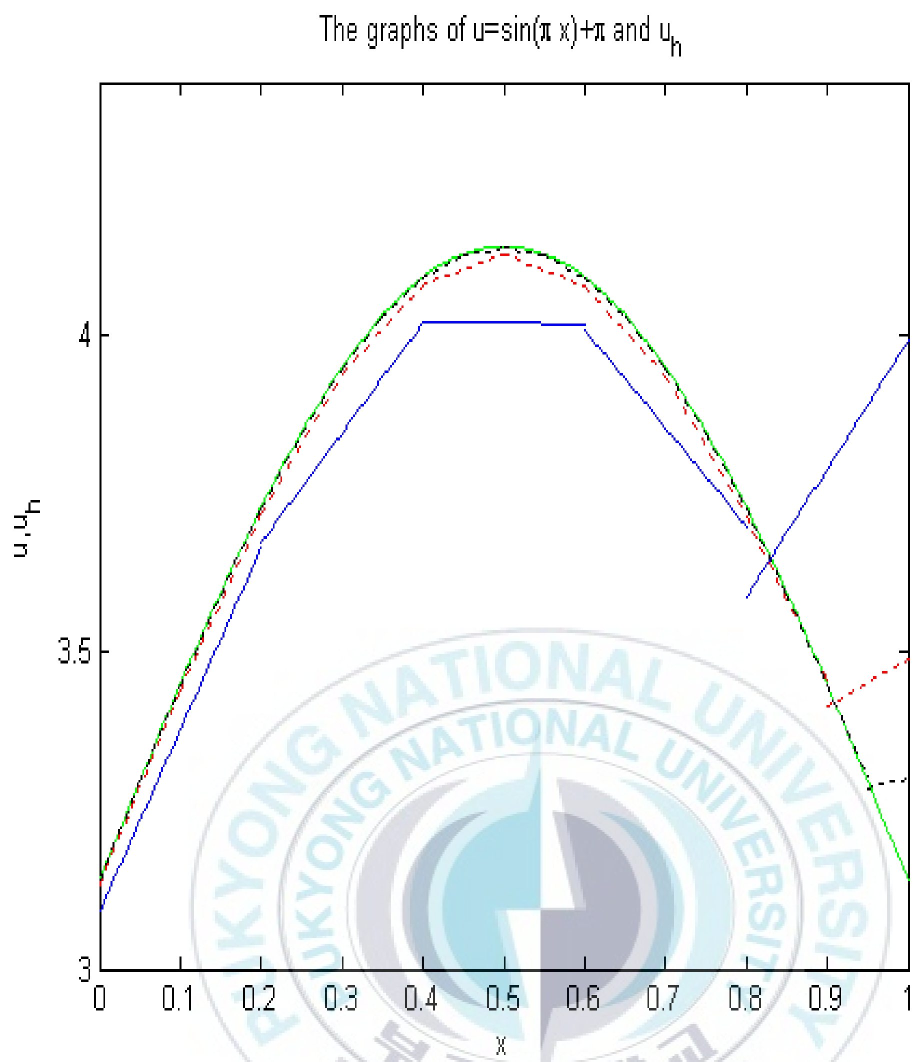

Figure 4.14. The graphs of the solution $u(x) = \sin(\pi x) + \pi$ and the approximate solution u_h in Case 2-1 when $p = 1$ and $h = 0.2, 0.1, 0.05$. The solid green line (the solution u), the solid blue line ($u_{0.2}$), the dotted red line ($u_{0.1}$), the dotted black line ($u_{0.05}$).

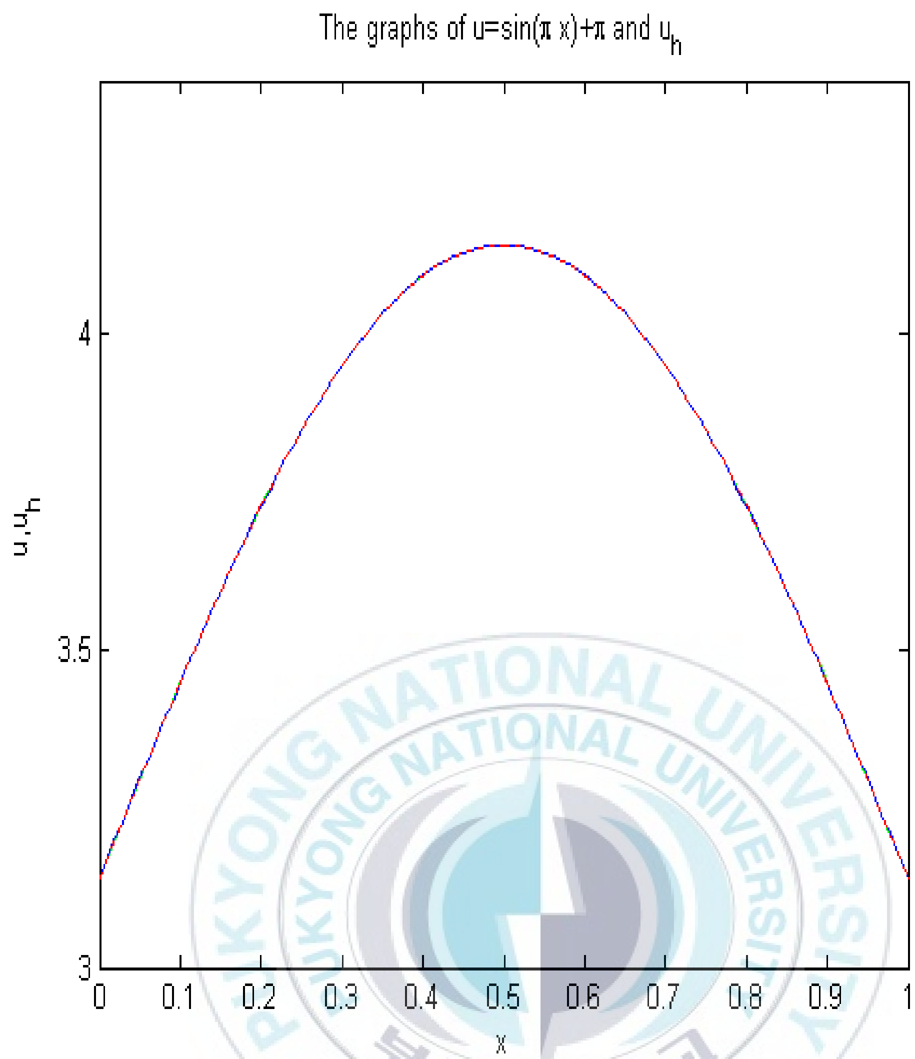

Figure 4.15. The graphs of the solution $u(x) = \sin(\pi x) + \pi$ and the approximate solution u_h in Case 2-1 when $p = 2$ and $h = 0.2, 0.1$. The solid green line (the solution u), the solid blue line ($u_{0.2}$), the dotted red line ($u_{0.1}$).

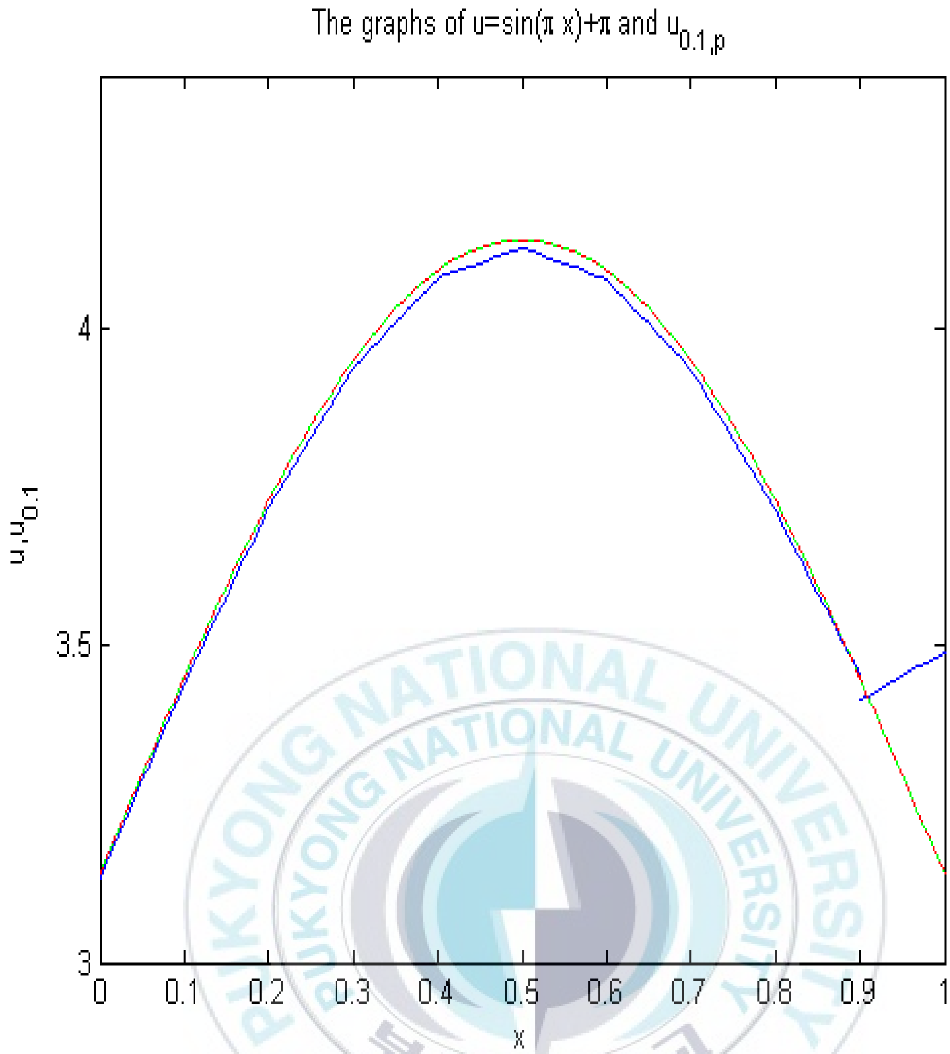

Figure 4.16. The graphs of the solution $u(x) = \sin(\pi x) + \pi$ and the approximate solution $u_{0.1,p}$ in Case 2-1 when $p = 1, 2$. The solid green line (the solution u), the solid blue line ($u_{0.1,1}$), the dotted red line ($u_{0.1,2}$).

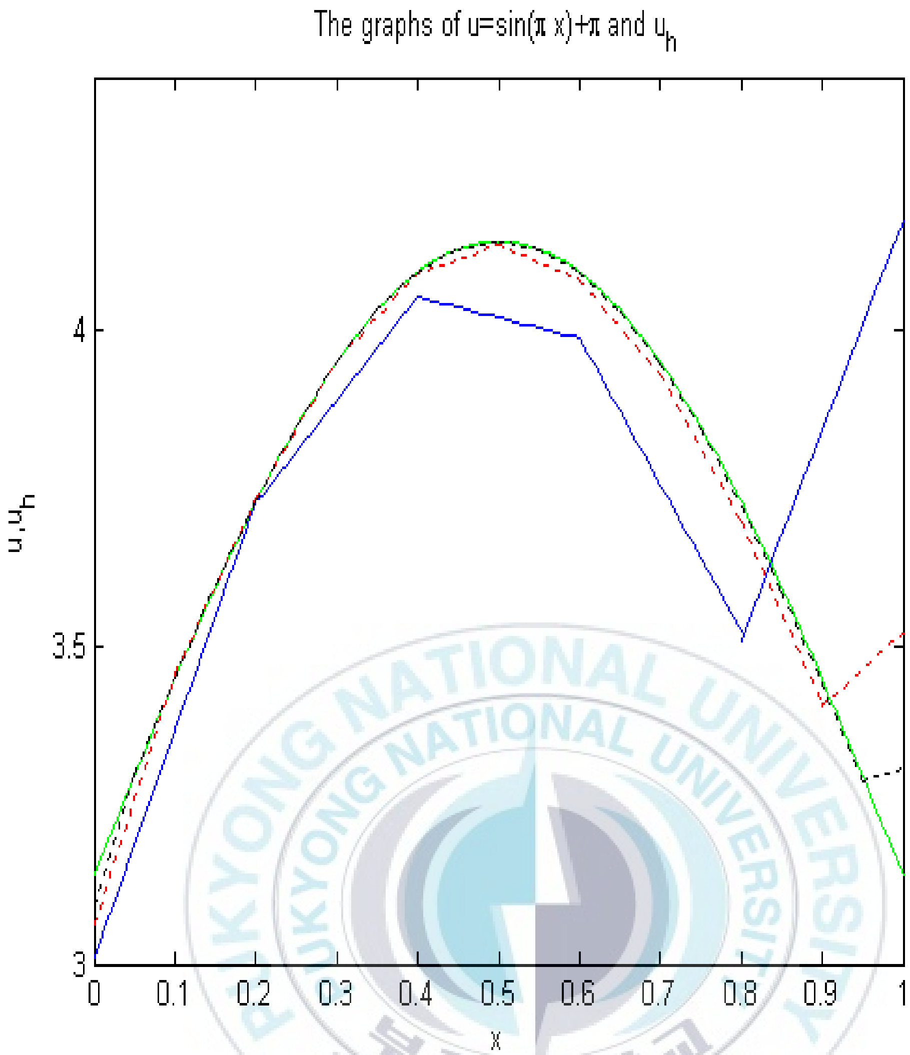

Figure 4.17. The graphs of the solution $u(x) = \sin(\pi x) + \pi$ and the approximate solution u_h in Case 2-2 when $p = 1$ and $h = 0.2, 0.1, 0.05$. The solid green line (the solution u), the solid blue line ($u_{0.2}$), the dotted red line ($u_{0.1}$), the dotted black line ($u_{0.05}$).

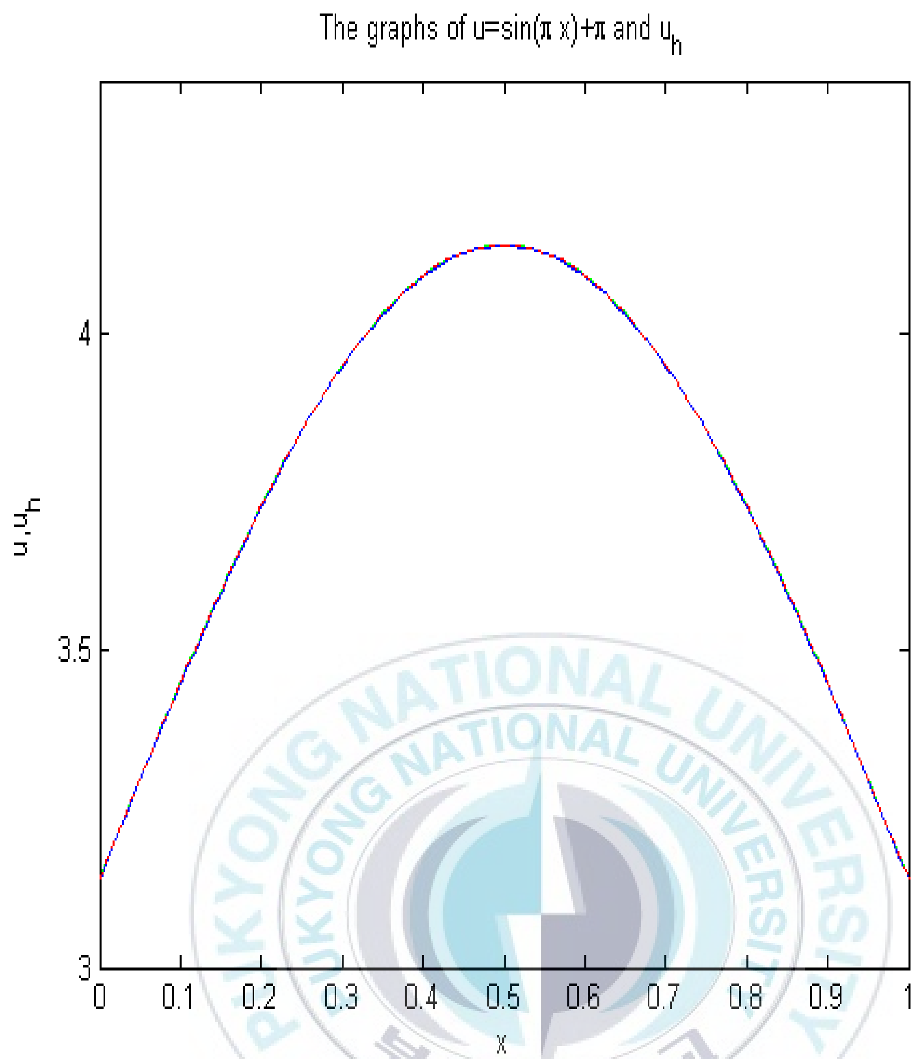

Figure 4.18. The graphs of the solution $u(x) = \sin(\pi x) + \pi$ and the approximate solution u_h in Case 2-2 when $p = 2$ and $h = 0.2, 0.1$. The solid green line (the solution u), the solid blue line ($u_{0.2}$), the dotted red line ($u_{0.1}$).

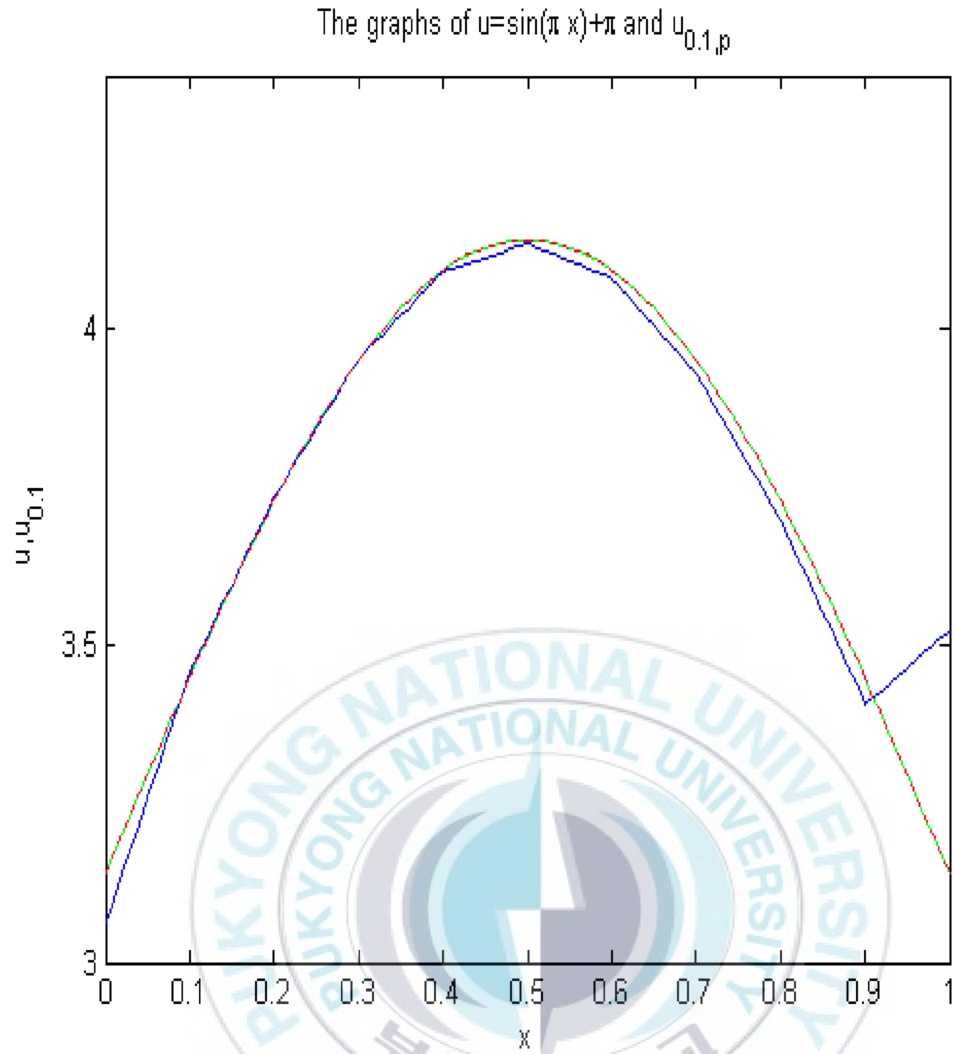

Figure 4.19. The graphs of the solution $u(x) = \sin(\pi x) + \pi$ and the approximate solution $u_{0.1,p}$ in Case 2-2 when $p = 1, 2$. The solid green line (the solution u), the solid blue line ($u_{0.1,1}$), the dotted red line ($u_{0.1,2}$).

Table 4.25. The computed L^2 norm of $u - u_h$ in Case 2-1: $p = 1, 2$, $u(x) = \sin(\pi x) + \pi$, $N = 5, 10, 20, 40, 80$.

N	p=1	p=2
5	2.225969606782825E-001	7.666019200147692E-004
10	6.616494882870272E-002	8.525429197474917E-005
20	2.204014562927687E-002	9.958587117385645E-006
40	7.616910129077757E-003	1.200208807141774E-006
80	2.667814632869868E-003	1.472098247661973E-007

Table 4.26. The computed L^2 norm of $u - u_h$ in Case 2-2: $p = 1, 2$, $u(x) = \sin(\pi x) + \pi$, $N = 5, 10, 20, 40, 80$.

N	p=1	p=2
5	2.617116864029930E-001	2.553209603894086E-003
10	7.002147178905178E-002	1.217649195356966E-004
20	2.245694781209066E-002	1.478781957367325E-005
40	7.799379182176414E-003	1.829844805572084E-006
80		2.277663477514139E-007

Table 4.27. Convergence rates of the computed L^2 norm of $u - u_h$ in Case 2-1 when $u(x) = \sin(\pi x) + \pi$.

N	p=1	p=2
5	1.75	3.17
10	1.59	3.10
20	1.53	3.05
40	1.51	3.03

Table 4.28. Convergence rates of the computed L^2 norm of $u - u_h$ in Case 2-2 when $u(x) = \sin(\pi x) + \pi$.

N	p=1	p=2
5	1.90	4.39
10	1.64	3.04
20	1.53	3.01
40		3.01

5. Conclusions

In this thesis, we introduce a discontinuous Galerkin method for the boundary value problem with the mixed boundary conditions and present the numerical results of the method - especially, the computed L^2 error of discontinuous Galerkin approximations and their convergence rates. The main results of this study are summarized as follows:

(1) For the boundary value problem

$$-\frac{d}{dx}\Big(a(\frac{du}{dx}+bu)\Big)+du=f, \quad \text{in } I=(0,1)$$

with the homogeneous Naumann boundary conditions

$$\frac{du}{dx}=0 \quad \text{at} \quad x=0 \text{ and } x=1 \text{ (provided that } b(0)=0 \text{ and } b(1)=0),$$

we know from the numerical experiments that the convergence rates of the computed L^2 norm of $u-u_h$ are $O(h^{p+1})$, where p denotes the degree of polynomials in V_h and $p=1,2$.

(2) For the boundary value problem

$$-\frac{d}{dx}\Big(a(\frac{du}{dx}+bu)\Big)+du=f, \quad \text{in } I=(0,1)$$

with the homogeneous mixed boundary conditions

$$\frac{du}{dx}+bu=0 \quad \text{at} \quad x=0 \text{ and } x=1 \text{ (provided that } b(0)\neq 0 \text{ and } b(1)\neq 0),$$

we also know from the numerical experiments that the convergence rates of the computed L^2 norm of $u - u_h$ are

$$O(h^{3/2}) \text{ when } p = 1 \quad \text{and} \quad O(h^3) \text{ when } p = 2$$

where p denotes the degree of polynomials in V_h.

Notice that the numerical results of this thesis give us some motivations for further theoretical studies on discontinuous Galerkin methods for the boundary value problem with the mixed boundary conditions. And notice that it is open problems to prove these numerical results theoretically.

References

[1] D.N. Arnold, *An interior penalty finite element method with discontinuous elements*, SIAM J. Numer. Anal. **19** no. 4 (1982), 742–760.

[2] D.N. Arnold, F. Brezzi, B. Cockburn, and L.D. Marini, *Unified analysis of discontinuous Galerkin methods for elliptic problems*, SIAM J. Numer. Anal. **39** no. 5 (2001/02), 1749–1779.

[3] I. Babuska, C.E. Baumann, and J.T. Oden, *A discontinuous hp finite element method for diffusion problems: 1-D analysis*, Comput. Math. Appl. **37** no. 9 (1999), 103–122.

[4] F. Brezzi, G. Manzini, D. Marini, P. Pietra, and A. Russo, *Discontinuous Galerkin approximations for elliptic problems*, Numer. Methods Partial Differential Equations **16** no. 4 (2000), 365–378.

[5] H. Chen, Z. Chen, and B. Li, *Numerical study of the hp version of mixed discontinuous finite element methods for reaction-diffusion problems: the 1D cases*, Numer. Methods Partial Differential Equations **19** no.4 (2003), 525-553.

[6] Z. Chen, *On the relationship of various discontinuous finite element methods for second-order elliptic equations*, East-West J. Numer. Math. **9** no.2 (2001), 99-122.

[7] B. Cockburn, G.E. Karniadakis, and C.-W. Shu, *Discontinuous Galerkin methods: Theory, computation and applications*, Lect. Notes Comput. Sci. Eng, 11. Springer-Verlag, Berlin, 2000.

[8] J. Douglas and T. Dupont, *Interior panalty procedures for elliptic and*

parabolic Galerkin methods, in: Lecture Notes in Phys. **58**, Springer, Berlin, (1976), 207-216.

[9] K. Harriman, P. Houston, B. Senior, and E. Süli, *hp-version discontinuous Galerkin methods with interior penalty for partial differential equations with nonnegative characteristic form*, In recent advances in scientific computing and partial differential equations, edited by C.-W. Shu, T. Tang, and S.-Y, Cheng, Contemp. Math., **330** (2003), 89-119.

[10] M.G. Larson and J. Niklasson, *Analysis of a familiy of discontinuous Galerkin methods for elliptic problems: the one dimensional case*, Numer. Math. **99** (2004), 113-130.

[11] J. A. Nitsche, *Uber ein Variationsppringzip zur Losung von Dirichlet-Problem bei Verwendung von Teilraumen, die keinen Randbedingungen unterworfen sind*, Abh. Math. Sem. Univ. Hamburg **36** (1971) 9-15.

[12] J.T. Oden, I. Babuska, and C.E. Baumann, *A discontinuous hp finite element method for diffusion problems*, J. Comput. Phys. **146** (1998), 103–122.

[13] S. Prudhomme, F. Pascal, J.T. Oden, and A. Romkes, *A priori error estimates for the Baumann-Oden version of the discontinuous Galerkin method*, C.R. Acad. Sci. Paris Ser. I Math. **332** no. 9 (2001), 851-856.

[14] B. Riviere, M.F. Wheeler, and V. Girault, *Improved energy estimates for interior penalty, constrained and discontinuous Galerkin methods for elliptic problems I*, J. Comput. Geosci. **3-4** (2000), 337-360.

[15] M.F. Wheeler, *An elliptic collocation-finite element method with interior penalties*, SIAM J. Numer. Anal. **15** no. 1 (1978), 152–161.